# Glycosylation and Membrane Stabilization
# MVIMIG 7470-March 6, 2014

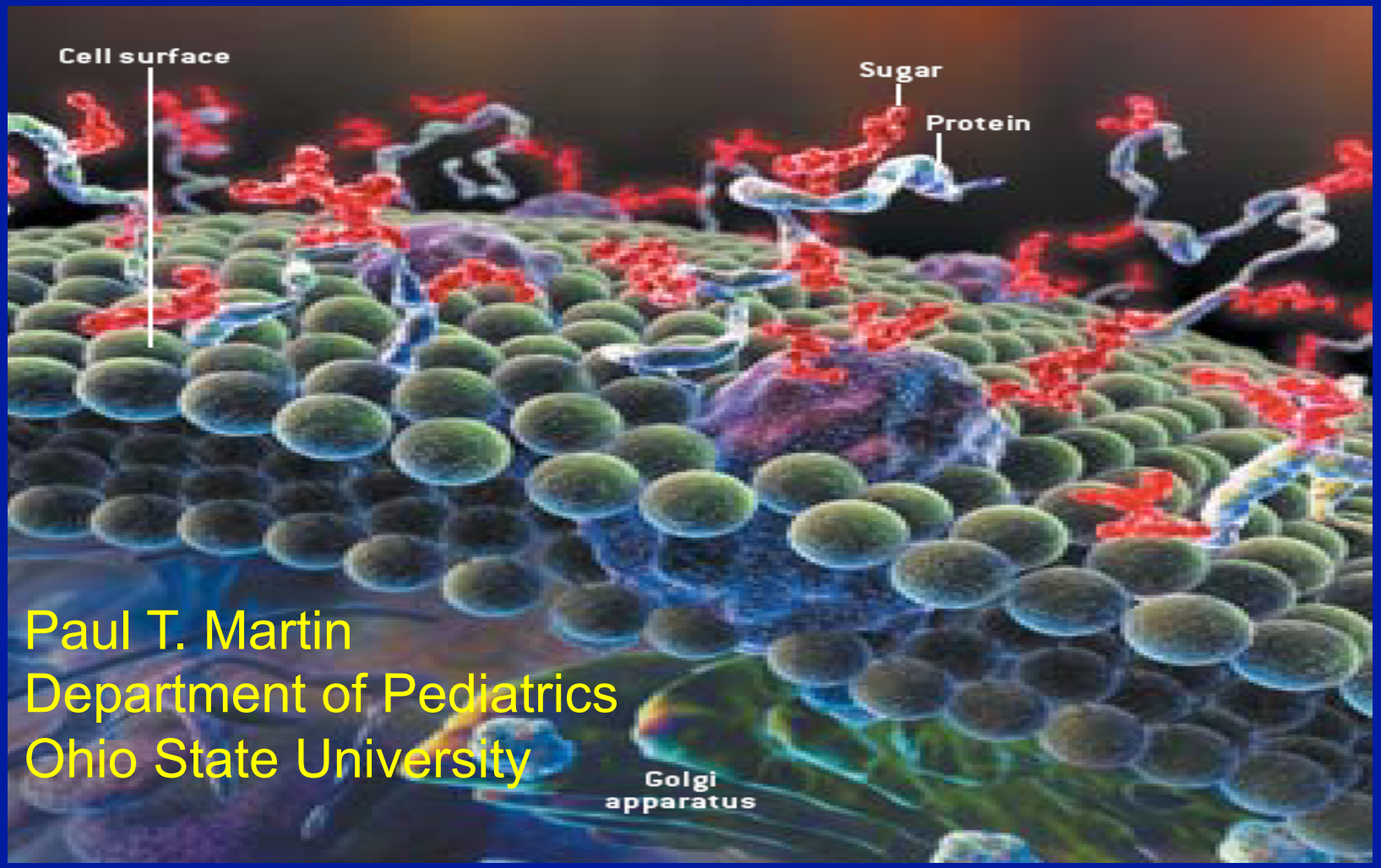


Paul T. Martin
Department of Pediatrics
Ohio State University

# The glycocalyx

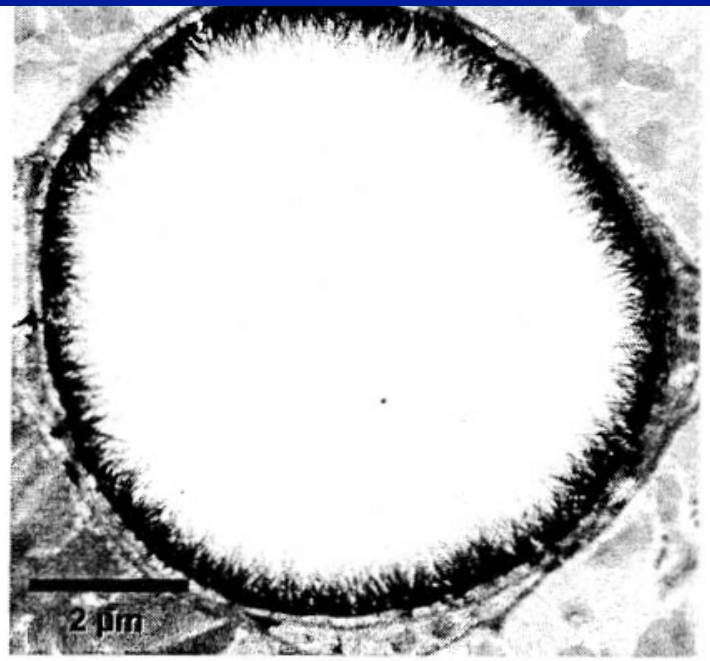


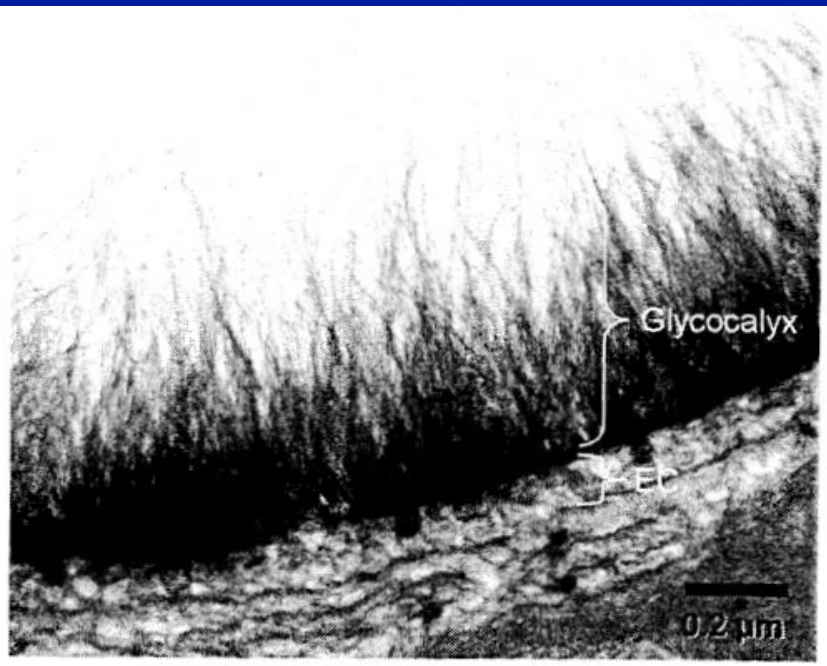


**Fig. 1.** Electron micrograph of a goat coronary capillary stained with

# Universal Characteristics of All Living Cells

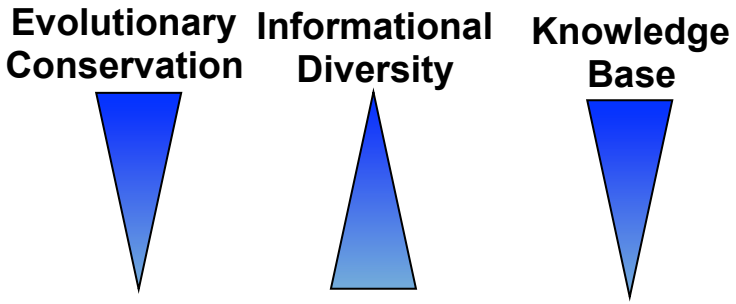


- Genetic Code Based on DNA (*Genome*)
- Diverse RNAs: mRNA, miRNAs etc. (*Transcriptome*)
- Structural and Functional Proteins (*Proteome*)
- Energy Flux and Signaling Molecules (*Metabolome*)
- Lipid-based Membranes (*Lipidome*)
- Cell Surface/Secreted/Intracellular Glycans (*Glycome*)

**Glycosylation is Universal to All Living Cells.**

**Evolution has Failed to Generate A Cell that is Devoid of Glycosylation.**

**Thus, Glycosylation is As Essential to Life as a Genetic Code!**

Modified from: Varki A. *Cold Spring Harbor Perspectives in Biology*, 2011

Based on Karolinska Institut 200th. Anniversary Symposium Lecture

# Potential Complexity of Macromolecules

| Macromolecule | Building Block | Aproximate Mass | Possible Variations in a Trimer |
|---|---|---|---|
| Protein | Amino acids | 125 → $10^4$-$10^5$ | |
| Nucleic Acid | Nucleotides | 330 → $10^3$-$10^9$ | |
| Lipid | Fatty acids | 250 → $10^3$ | |
| Carbohydrate<br><br>(Glycan) | Monosaccharides | 200 → $10^2$-$10^6$ | |

**Further complexity in glycans generated by Alpha/ Beta linkages and by branching**

# Common classes of animal glycans

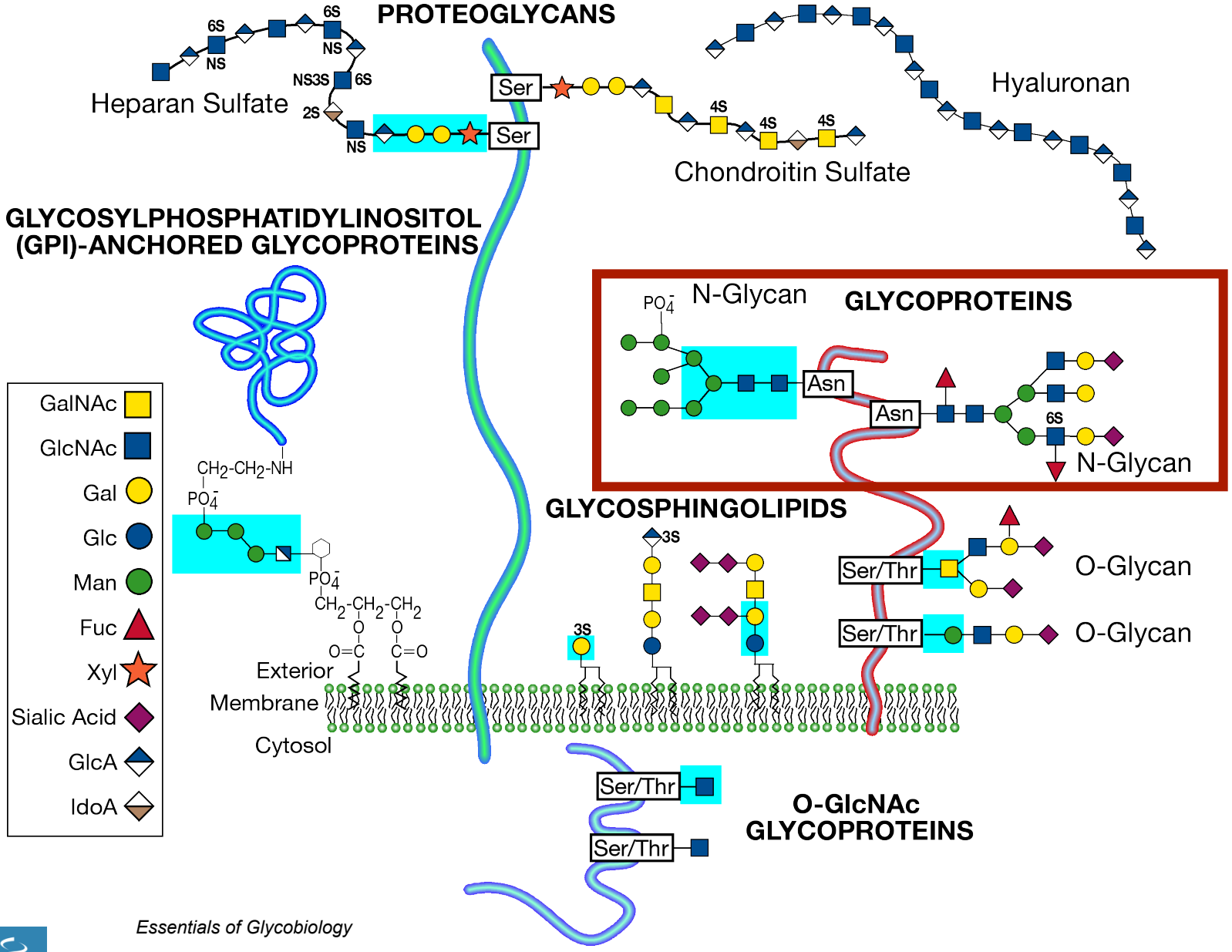


*Essentials of Glycobiology*

Second
Edition

# Common classes of animal glycans

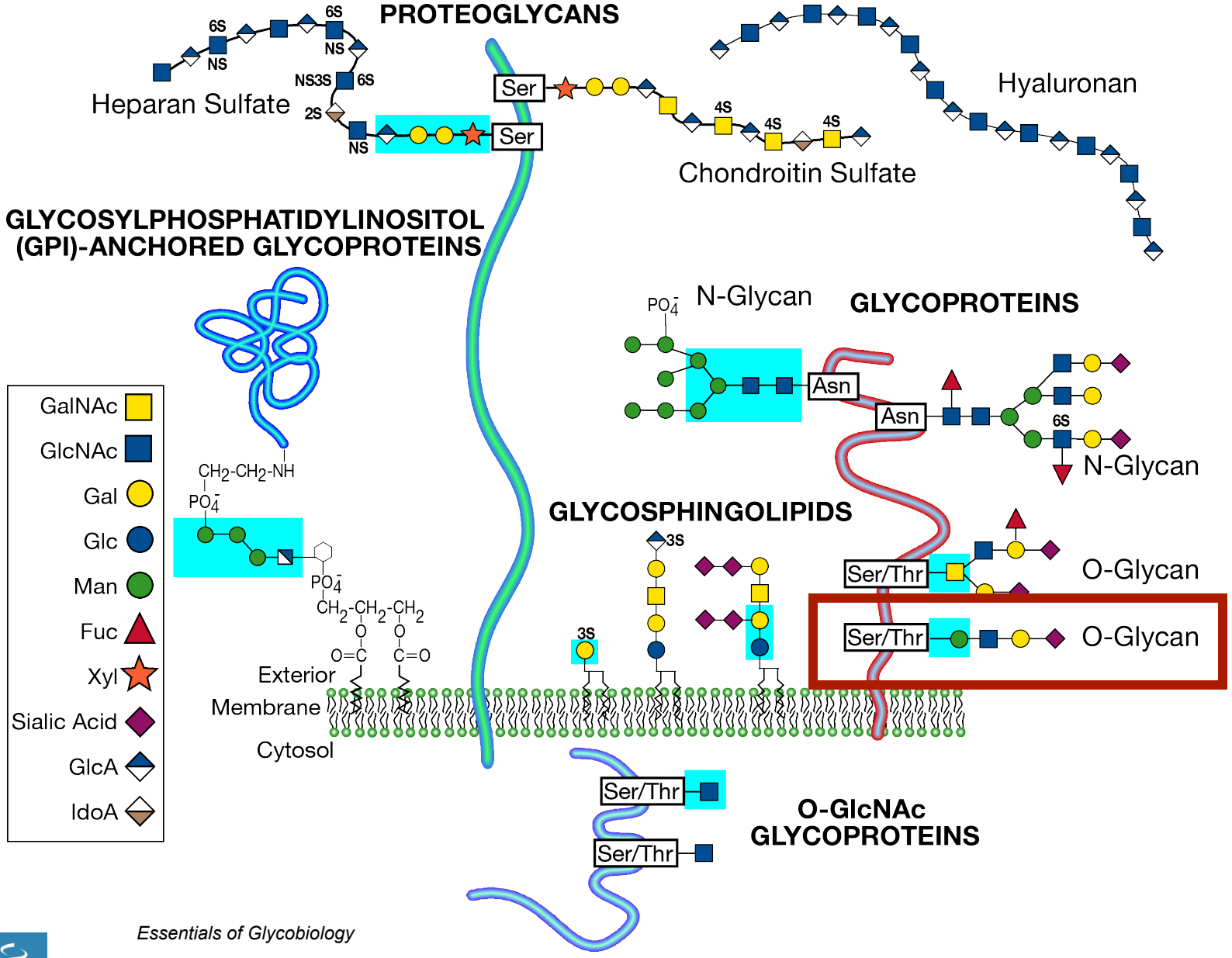


*Essentials of Glycobiology*

Second
Edition

# The N-linked pathway and associated CDGs

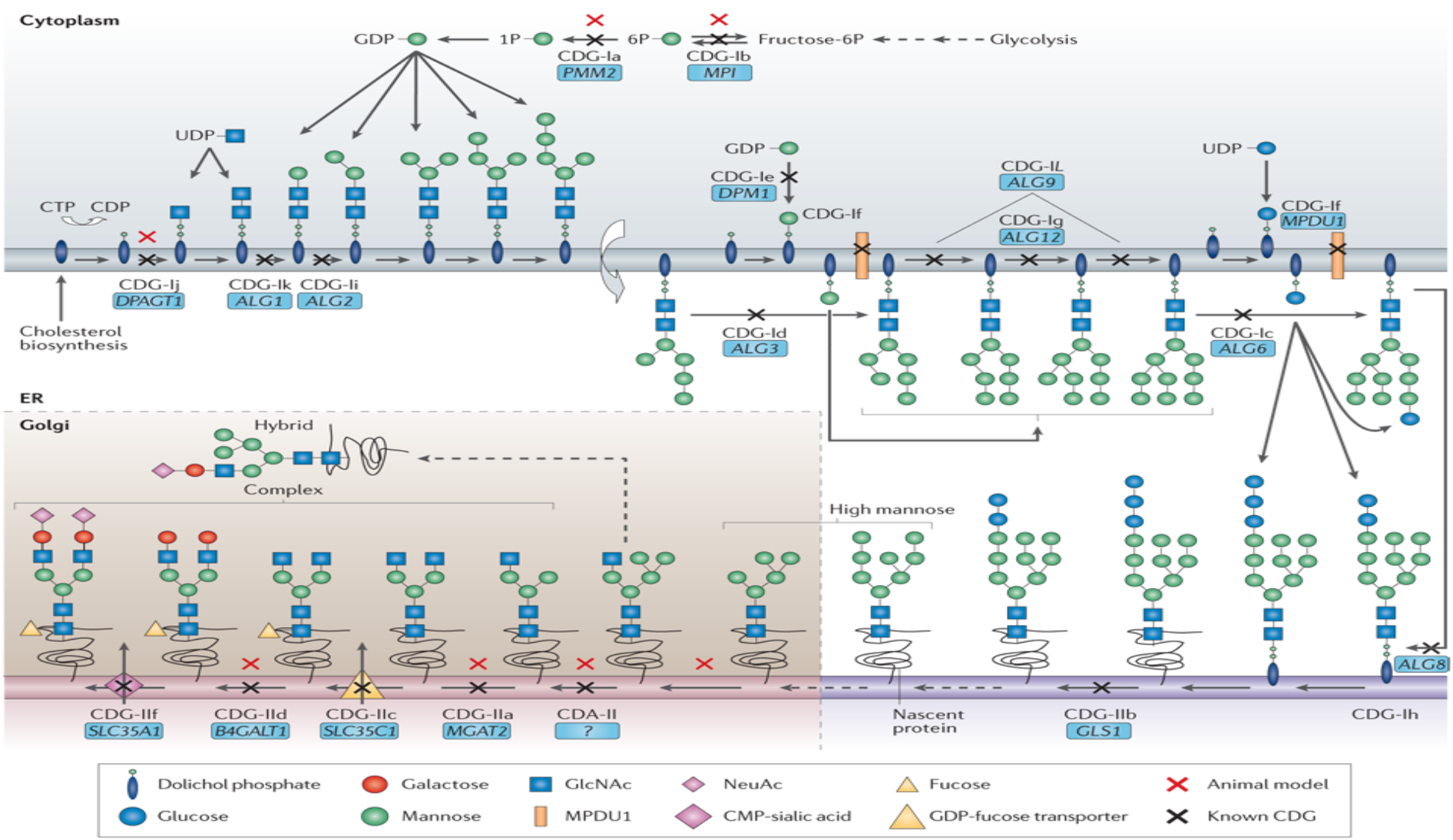


Figure 3 | **Sites of genetic defects in the *N*-linked glycan biosynthetic pathway.** During *N*-linked glycan biosynthesis, monosaccharides of GlcNAc (*N*-acetylglucosamine) and mannose are activated or interconverted and used to build the lipid-linked oligosaccharide precursor (LLO), which is assembled on dolichol, a polyisoprenoid that is derived

# DPK and DPM1,2,3 Complex

Lefeber et al. 2009 *Am. J. Hum. Genet.* 85, 76

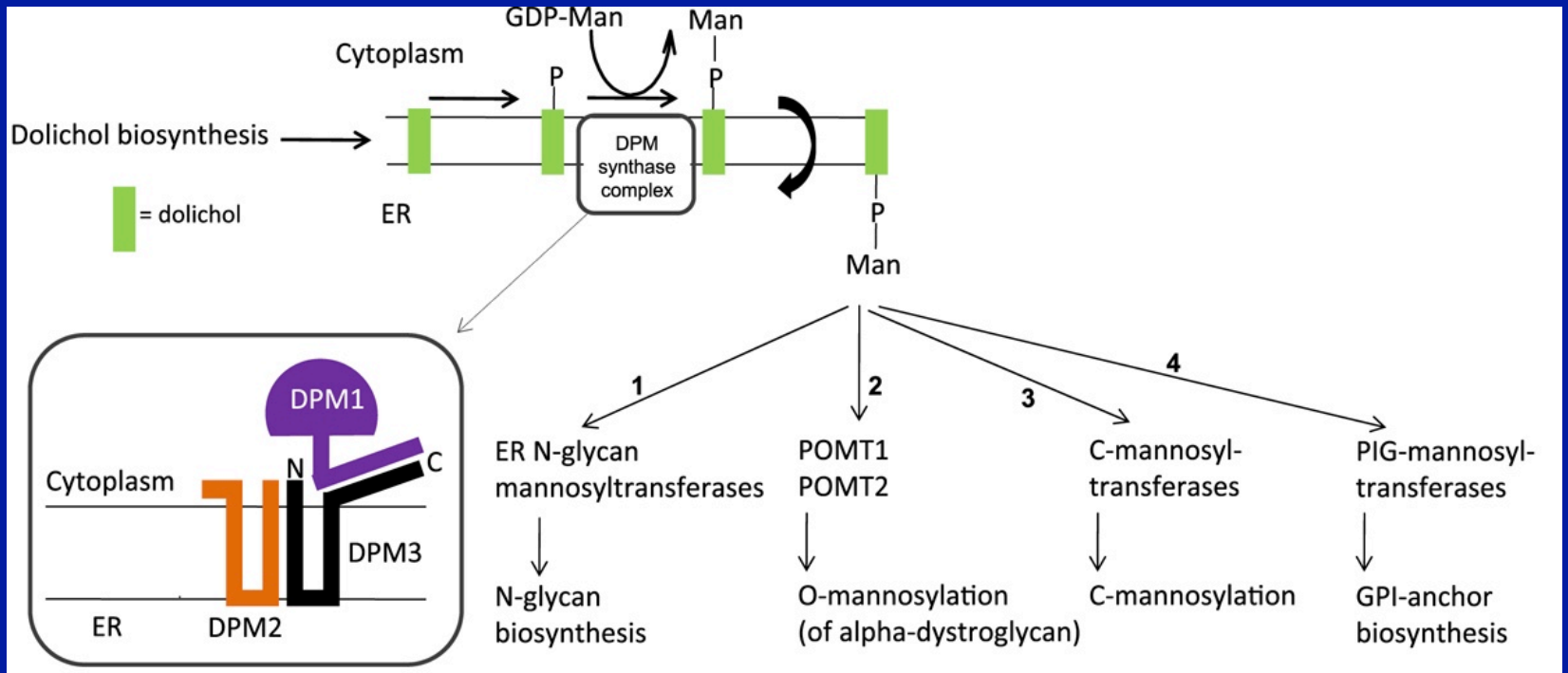


**Figure 1. Architecture of the Dol-P-Man Synthase Complex**

The enzymatically active DPM1 subunit in the cytoplasm is anchored to subunits DPM2 and DPM3 in the ER membrane via the C-terminal peptide of DPM3. Four biosynthetic pathways depend on Dol-P-Man: N-glycosylation (1), O-mannosylation (2), C-Mannosylation (3), and GPI-anchor biosynthesis (4).

Table 2 | **Human diseases caused by genetic defects in *N*-glycosylation pathways**

| Disorder | Gene | Enzyme | OMIM | Key Features |
|---|---|---|---|---|
| CDG-Ia | *PMM2* | Phosphomannomutase II | 212065 | Mental retardation, hypotonia, esotropia, lipodystrophy, cerebellar hypoplasia, stroke-like episodes, seizures |
| CDG-Ib | *MPI* | Phosphomannose isomerase | 602579 | Hepatic fibrosis, protein-losing enteropathy, coagulopathy, hypoglycaemia |
| CDG-Ic | *ALG6* | Glucosyltransferase I Dol-P-Glc: $Man_9$-$GlcNAc_2$-P-P-Dol glucosyltransferase | 603147 | Moderate mental retardation, hypotonia, esotropia, epilepsy |
| CDG-Id | *ALG3* | Dol-P-Man:$Man_5$-$GlcNAc_2$-P-P-Dol mannosyltransferase | 601110 | Profound psychomotor delay, optic atrophy, acquired microcephaly, iris colobomas, hypsarrhythmia |
| CDG-Ie | *DPM1* | Dol-P-Man synthase I GDP-Man: Dol-P-mannosyltransferase | 603503 | Severe mental retardation, epilepsy, hypotonia, mild dysmorphism, coagulopathy |
| CDG-If | *MPDU1* | Man-P-Dol utilization 1/Lec35 | 608799 | Short stature, icthyosis, psychomotor retardation, pigmentary retinopathy |
| CDG-Ig | *ALG12* | Dol-P-Man:$Man_7$-$GlcNAc_2$P-P-Dol mannosyltransferase | 607143 | Hypotonia, facial dysmorphism, psychomotor retardation, acquired microcephaly, frequent infections |
| CDG-Ih | *ALG8* | Glucosyltransferase II Dol-P-Glc: $Glc_1$-$Man_9$-$GlcNAc_2$-P-P-Dol glucosyltransferase | 608104 | Hepatomegaly, protein-losing enteropathy, renal failure, hypoalbuminaemia, oedema, ascites |
| CDG-Ii | *ALG2* | Mannosyltransferase II GDP-Man: $Man_1$-$GlcNAc_2$-P-P-Dol mannosyltransferase | 607906 | Normal at birth; mental retardation, hypomyelination, intractable seizures, iris colobomas, hepatomegaly, coagulopathy |
| CDG-Ij | *DPAGT1* | UDP-GlcNAc: Dol-P-GlcNAc-P transferase | 608093 | Severe mental retardation, hypotonia, seizures, microcephaly, exotropia |
| CDG-Ik | ALG1 | Mannosyltransferase I GDP-Man: $GlcNAc_2$-P-P-Dol mannosyltransferase | 608540 | Severe psychomotor retardation, hypotonia, acquired microcephaly, intractable seizures, fever, coagulopathy, nephrotic syndrome, early death |
| CDG-Il | *ALG9* | Mannosyltransferase Dol-P-Man: $Man_6$- and $Man_8$-$GlcNAc_2$-P-P-Dol mannosyltransferase | 608776 | Severe microcephaly, hypotonia, seizures, hepatomegaly |
| CDG-IIa | *MGAT2* | GlcNAc transferase 2 | 212066 | Mental retardation, dysmorphism, stereotypies, seizures |
| CDG-IIb | *GLS1* | Glucosidase I | 606056 | Dysmorphism, hypotonia, seizures, hepatomegaly, hepatic fibrosis; death at 2.5 months |
| CDG-IIc | *SLC35C1/ FUCT1* | GDP-fucose transporter | 266265 | Recurrent infections, persistent neutrophilia, mental retardation, microcephaly, hypotonia; normal transferrin |
| CDG-IId | *B4GALT1* | β1,4 galactosyltransferase | 607091 | Hypotonia (myopathy), spontaneous haemorrhage, Dandy–Walker malformation |
| CDG-IIe | *COG7* | Conserved oligomeric Golgi complex subunit 7 | 608779 | Fatal in early infancy; dysmorphism, hypotonia, intractable seizures, hepatomegaly, progressive jaundice, recurrent infections, cardiac failure |
| CDG-IIf | *SLC35A1* | CMP-sialic acid transporter | 605634 | Thrombocytopaenia, no neurological symptoms; normal transferrin, abnormal platelet glycoproteins |
| CDG-II/COG1 | COG1 | Conserved oligomeric Golgi complex subunit 1 | 606973 | Hypotonia, growth retardation, progressive microcephaly, hepatosplenomegaly, mild mental retardation |
| Mucolipidosis II and III | *GNPTA* | UDP-GlcNAc: lysosomal enzyme, GlcNAc-P transferase | 252500 | Coarsening features, organomegaly, joint stiffness, dysostosis, median neuropathy at the wrist; MLIII is less severe than MLII, which presents in infancy |
| Congenital dyserythropoietic anaemia (CDA II) | Unknown | Unknown | 224100 | Anaemia, jaundice, splenomegaly, gall bladder disease |

CDG, congenital disorders of glycosylation; Dol, dolichol; Glc, glucose; GlcNAc, *N*-acetylglucosamine; Man, mannose.

# The Dystrophin-Associated Glycoprotein (DAG) complex

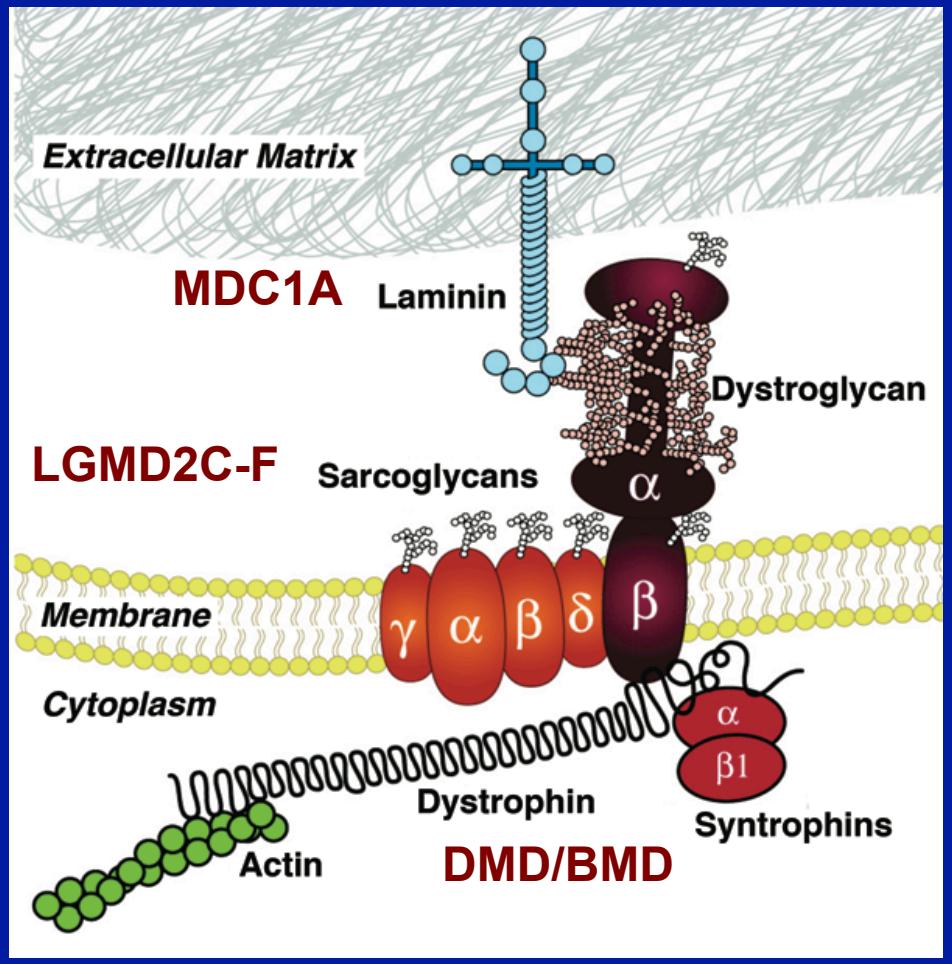


Ervasti et al.
1993 *J. Cell Biol.*
122, 809

# Dystroglycanopathies
# Congenital and Limb Girdle Muscular Dystrophies

Genes

*POMT1*
*POMT2*
*POMGnT1*
*Fukutin (FCMD)*
*Fukutin-related Protein (FKRP)*
*LARGE$^{myd}$*
*DAG1*
*DOLK*
*DPM1,2, 3*
*GTDC2/AG061*
*GMPPB*
*TMEM5*
*ISPD*
*B3GNT1*
*B3GALNT2*
*SGK196*

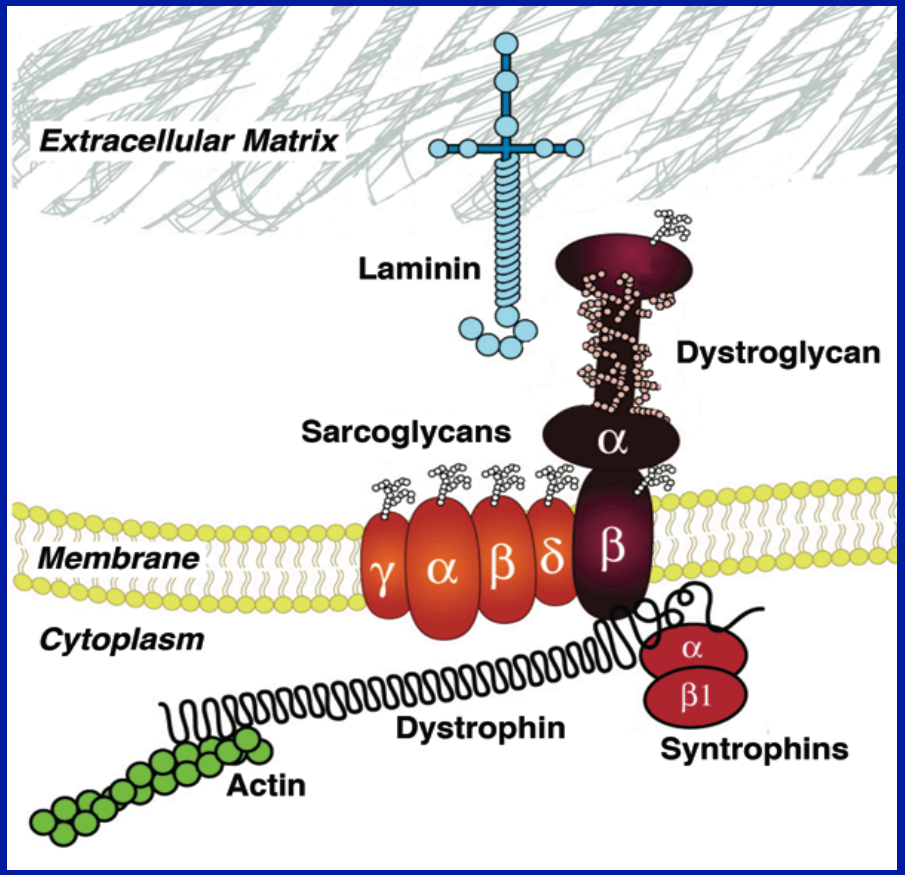


Diseases

WWS
MEB
FCMD
MCD1C
MCD1D
LGMD2I
LGMD2K
LGMD2L
LGMD2M
LGMD2N

GalNAcβ1,3GlcNAcβ1,4Man(6PO$_4$)α-

GlcNAcβ1,3Galβ1,4

Xylα1,3GlcAβ1,3

Neu5Ac/Gcα2,3Galβ1,4GlcNAcβ1,2Manα-O-Ser/Thr

# IIH6, a glycosylation-dependent function blocking mAB

## (Michele et al. 2002 *Nature* 418,417)

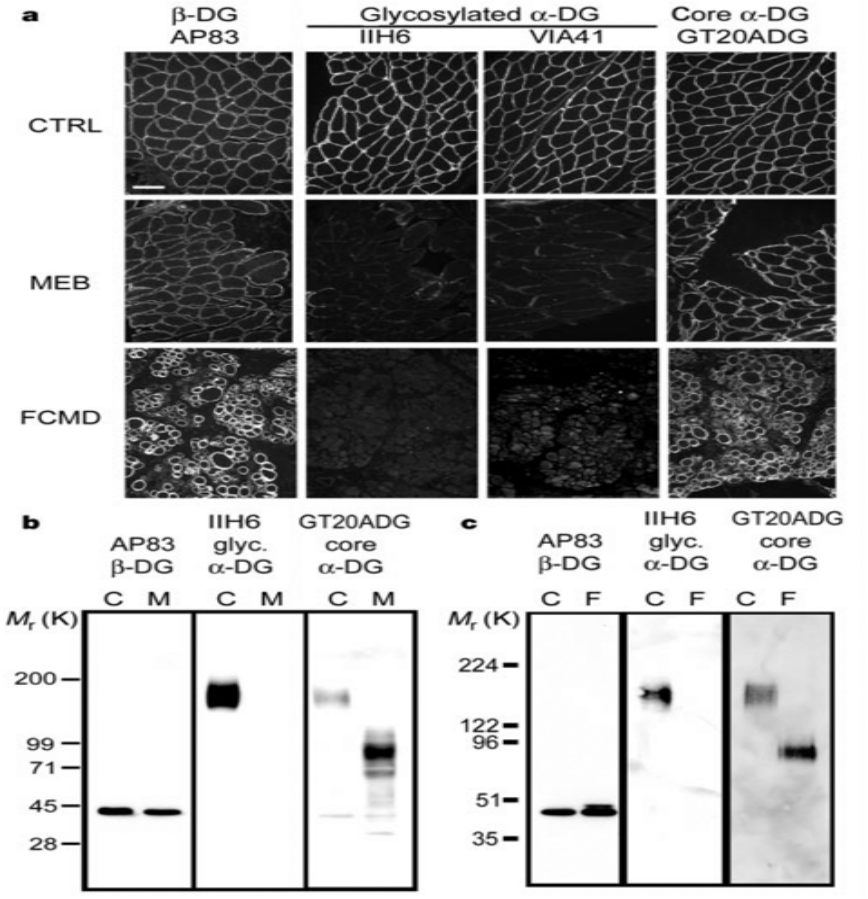


**Figure 1** Post-translational modification of dystroglycan in MEB and FCMD. **a**, Immunofluorescence localization of dystroglycan in biopsies of normal muscle (CTRL) and muscle of MEB and FCMD patients, using antibodies against β-DG, glycosylated α-DG, and α-DG core protein. Data shown are representative of all four MEB and all three FCMD patients. Scale bar, 100 μm. **b**, **c**, Immunoblot analyses of age-matched normal (C) and MEB patient (M, **b**) and FCMD patient (F, **c**) WGA-enriched total muscle glycoproteins.

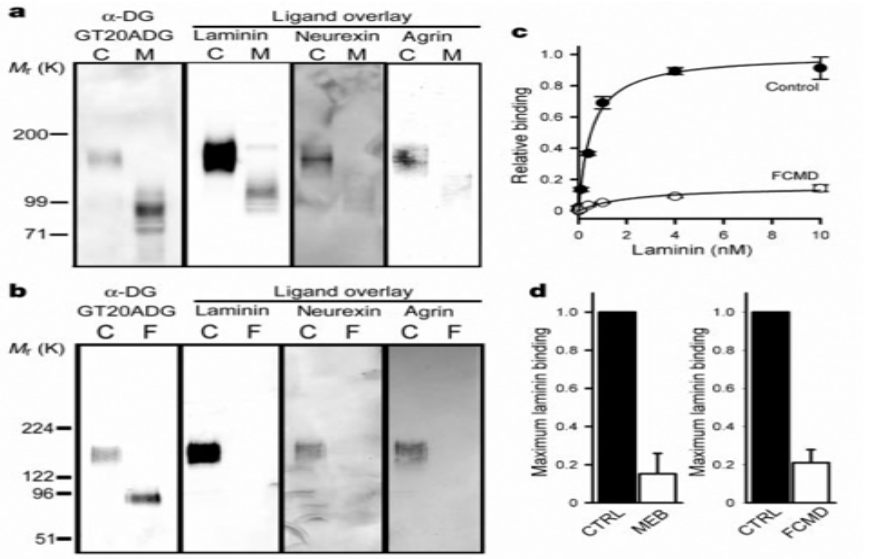


**Figure 2** Dystroglycan–ligand interactions in MEB and FCMD. **a**, **b**, Ligand overlay assays on age-matched control (C) and MEB patient (M, **a**) and FCMD (F, **b**) WGA-enriched muscle homogenates using murine EHS laminin, neurexin fusion protein and recombinant rat agrin. **c**, Representative assay of solid-phase laminin-binding activity from control and FCMD muscle. Data are mean ± s.d. of triplicate samples fitted to a one-site model using the equation $A = B_{max}x/(K_d + x)$. **d**, Maximum laminin-binding activity in MEB ($n = 2$) and FCMD ($n = 3$) WGA glycoproteins relative to age-matched control muscle (CTRL). Data are mean ± s.e.m.

# Reduced expression of αDG glycosylation in pediatric cancers (RMS)

LT Martin et al. (2007) *Hum. Pathol.* 38, 1657-68

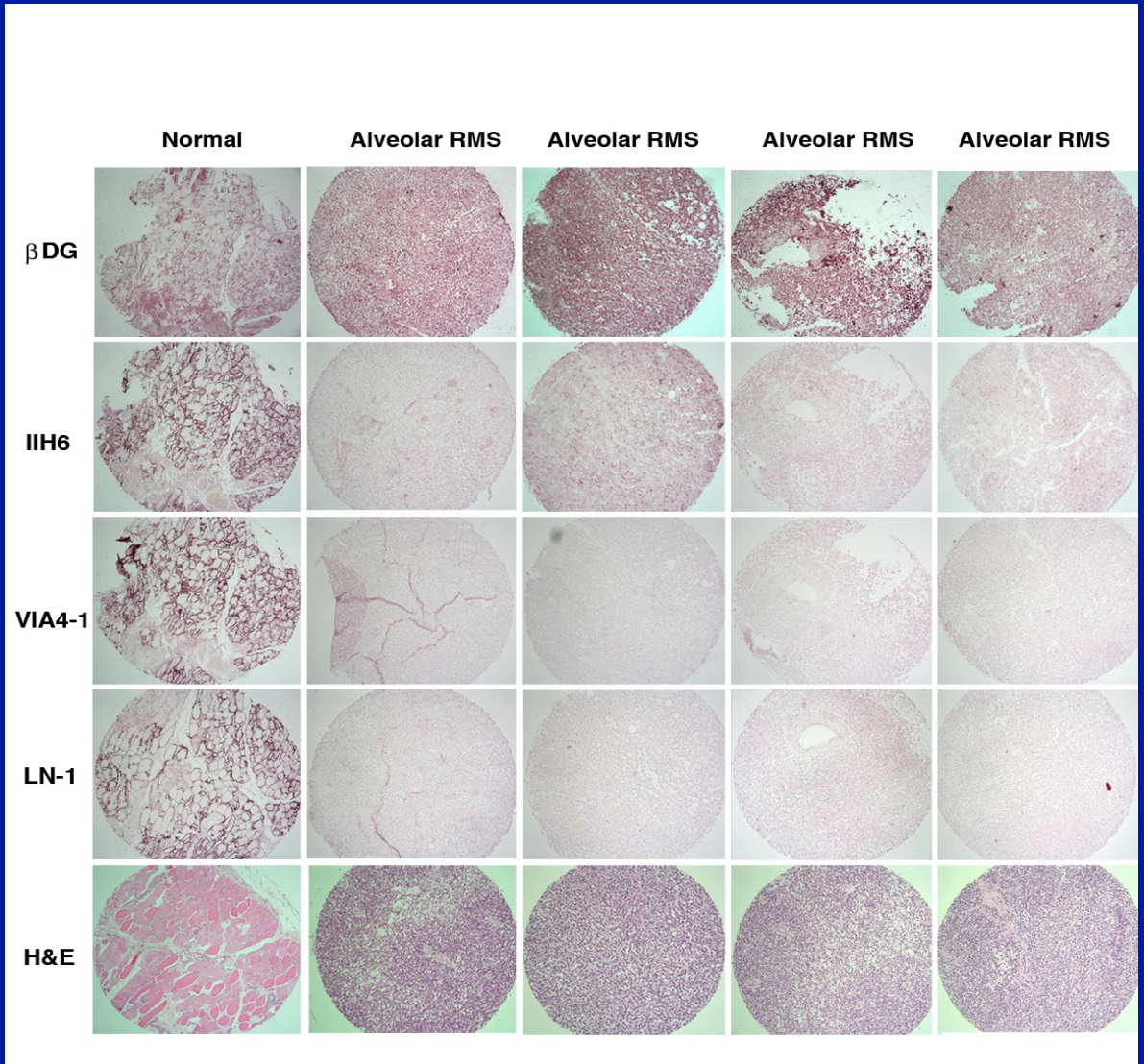

# Reduced αDG glycosylation (with or without reduced βDG) correlates with worsened tumor stage and survival

- Breast
- Prostate
- Colon

- Eosophogeal
- Pancreatic

- Rhabdomyosarcoma
- Neuroblastoma
- Medulloblastoma

# Multiple O-mannose-linked glycans on alpha DG

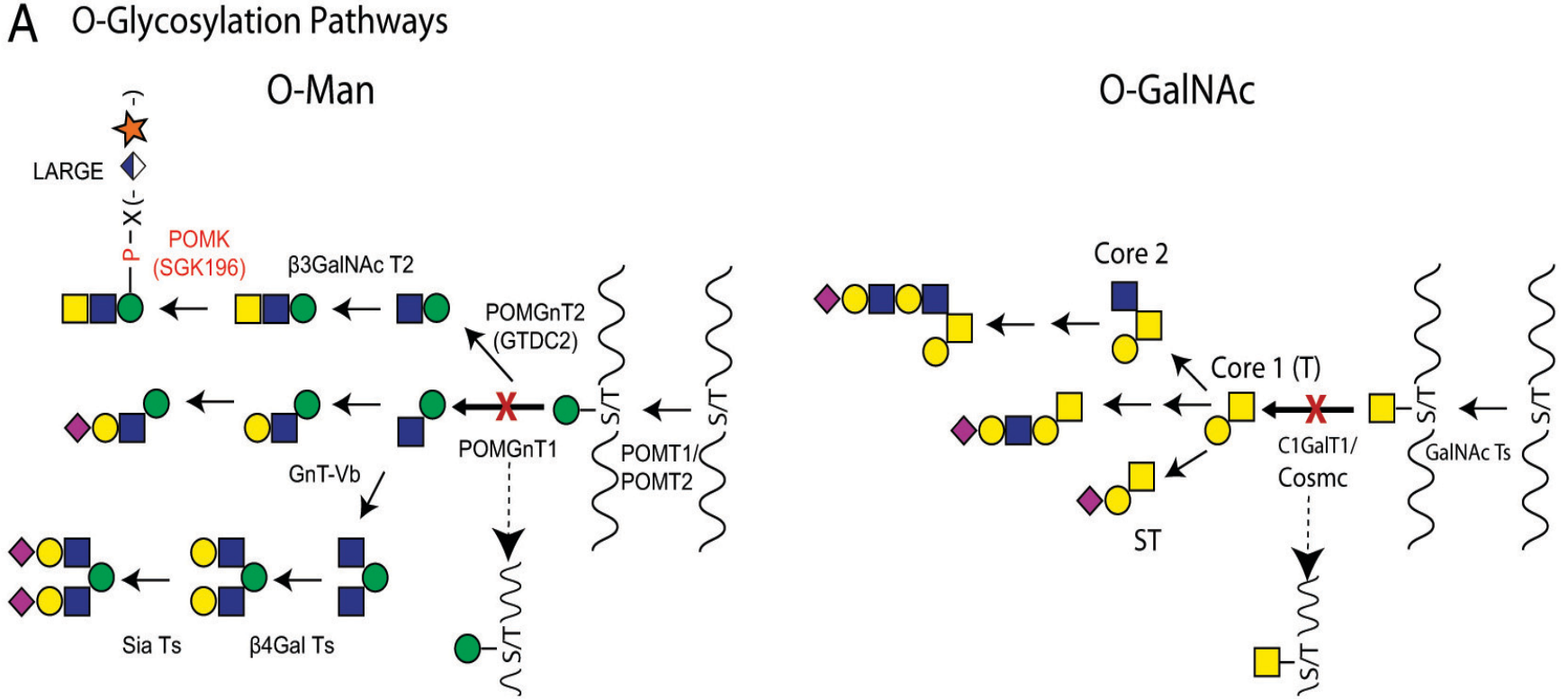


From Vester-Christensen et al. (2013) *Proc. Natl. Acad. Sci USA* **110**, 21018

# Glycans made by LARGE are sufficient to generate high affinity laminin binding

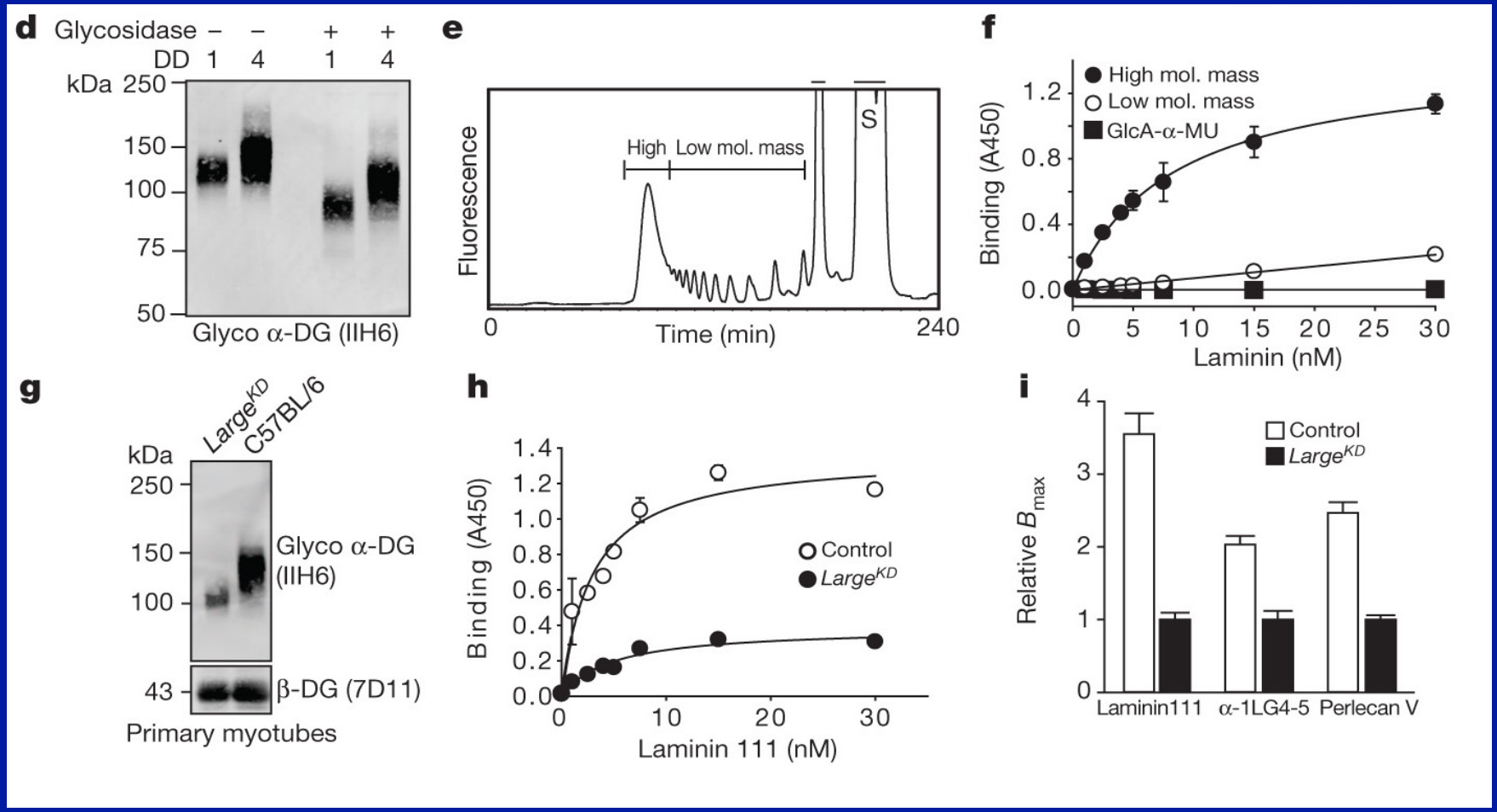


Goddeeris et al. (2013) *Nature* **503**, 136

# Are CMD cellular defects dystroglycan-specific?

- Glycosyltransferases usually alter glycosylation of multiple substrate proteins and lipids
- In this instance, one can phenocopy dystroglycanopathies by making DAG1-KO cells *in vivo* (Moore et al. 2002 *Nature* 418, 422; Cohn et al 2002 *Cell* 110(5), 639)
- Other proteins, however, are glycosylated by these disease genes (Feizi, Chai et al. 1999 *Eur. J. Biochem.* 263, 879)

# O-linked mannose structures are the same in Dag1-deficient brain

Stalnaker et al. 2011
J. Biol. Chem. 286, 21180

Other O-Man Proteins: E-cadherin, CD24, PTPRZ1, neurofascin 186, neurocan, versican

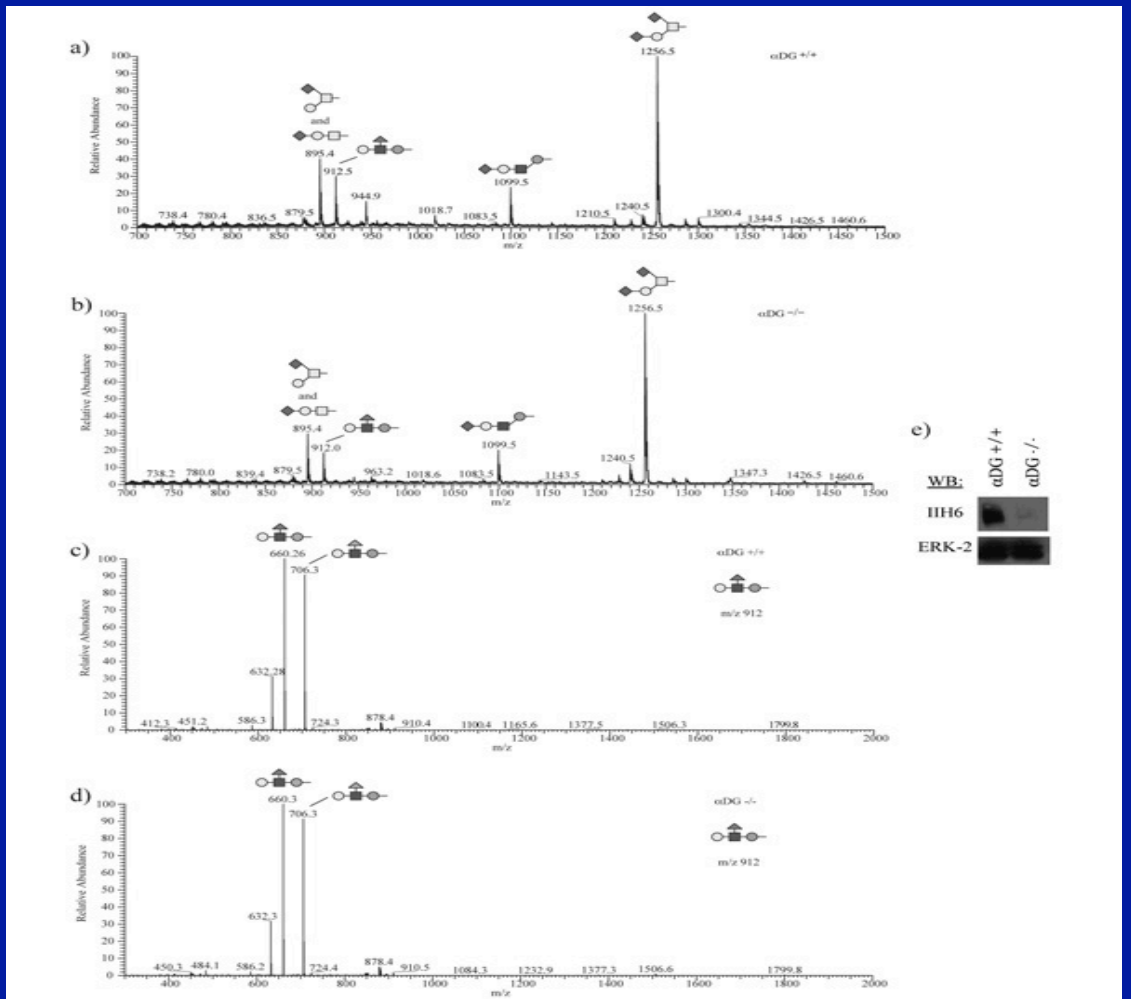


FIGURE 4. **O-Glycans released from α-DG$^{+/+}$ and α-DG$^{-/-}$ (GFAP-Cre/DAG1) mouse brain proteins.** *a* and *b*, *O*-glycans were released from protein powder of α-DG$^{+/+}$ and α-DG$^{-/-}$ cerebrums. Through comparison of the full scan, we observed no difference in the amount of prominent *O*-mannose-initiated glycan structures detected in the α-DG$^{+/+}$ and α-DG$^{-/-}$ proteins. *c* and *d*, MS/MS fragmentation spectra (*m/z* 912) indicate the presence of the fucosylated *O*-mannose trisaccharide structure in both the α-DG$^{+/+}$ and α-DG$^{-/-}$ mouse brains. *e*, antibody IIH6, which recognizes the fully glycosylated, functionally active form of α-DG, indicates an order of magnitude decrease in the amount of α-DG levels present in the α-DG$^{-/-}$ brain compared with the α-DG$^{+/+}$ brain. *WB*, Western blot.

# New, more clinically-driven, definition of dystroglycanopathy subtypes

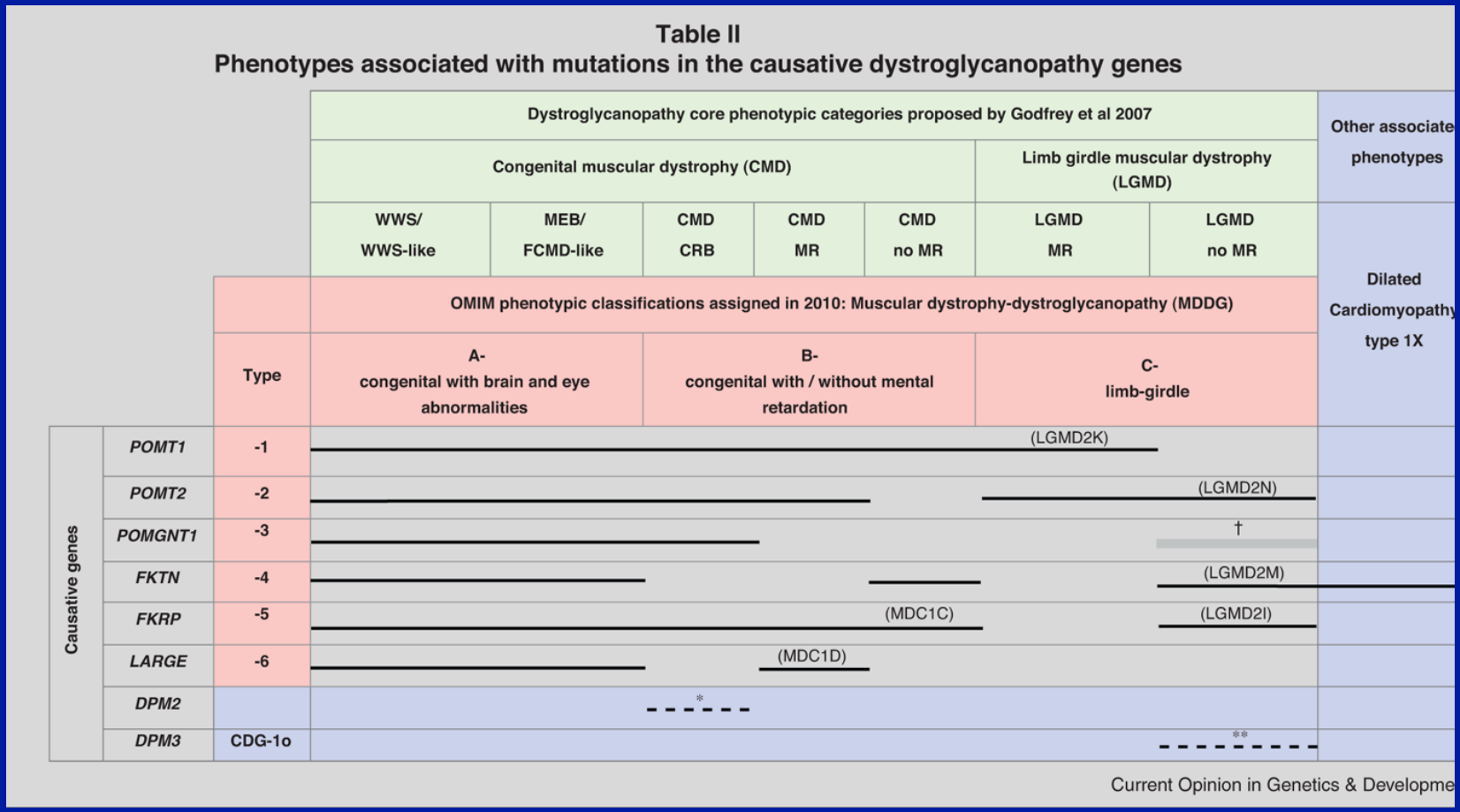

**Table II**
**Phenotypes associated with mutations in the causative dystroglycanopathy genes**

| | | | Dystroglycanopathy core phenotypic categories proposed by Godfrey et al 2007 | | | | | | | Other associate phenotypes |
|---|---|---|---|---|---|---|---|---|---|---|
| | | | Congenital muscular dystrophy (CMD) | | | | | Limb girdle muscular dystrophy (LGMD) | | |
| | | | WWS/ WWS-like | MEB/ FCMD-like | CMD CRB | CMD MR | CMD no MR | LGMD MR | LGMD no MR | |
| | | | OMIM phenotypic classifications assigned in 2010: Muscular dystrophy-dystroglycanopathy (MDDG) | | | | | | | Dilated Cardiomyopathy type 1X |
| | | Type | A- congenital with brain and eye abnormalities | | B- congenital with / without mental retardation | | | C- limb-girdle | | |
| Causative genes | *POMT1* | -1 | | | | | | (LGMD2K) | | |
| | *POMT2* | -2 | | | | | | | (LGMD2N) | |
| | *POMGNT1* | -3 | | | | | | | † | |
| | *FKTN* | -4 | | | | | | | (LGMD2M) | |
| | *FKRP* | -5 | | | | (MDC1C) | | | (LGMD2I) | |
| | *LARGE* | -6 | | | | (MDC1D) | | | | |
| | *DPM2* | | | | * | | | | | |
| | *DPM3* | CDG-1o | | | | | | | ** | |

Current Opinion in Genetics & Developme

# Walker-Warburg Syndrome (WWS)

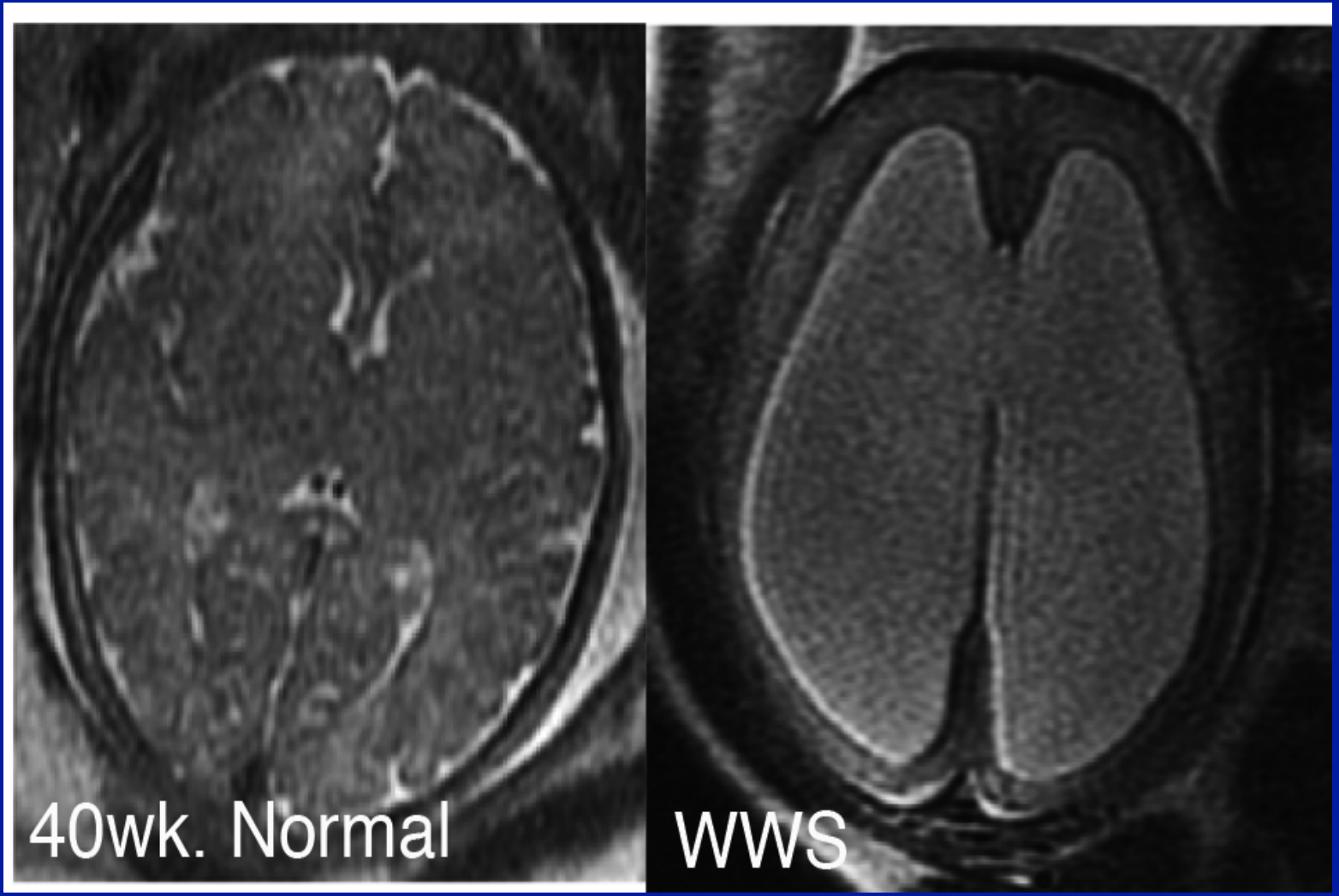

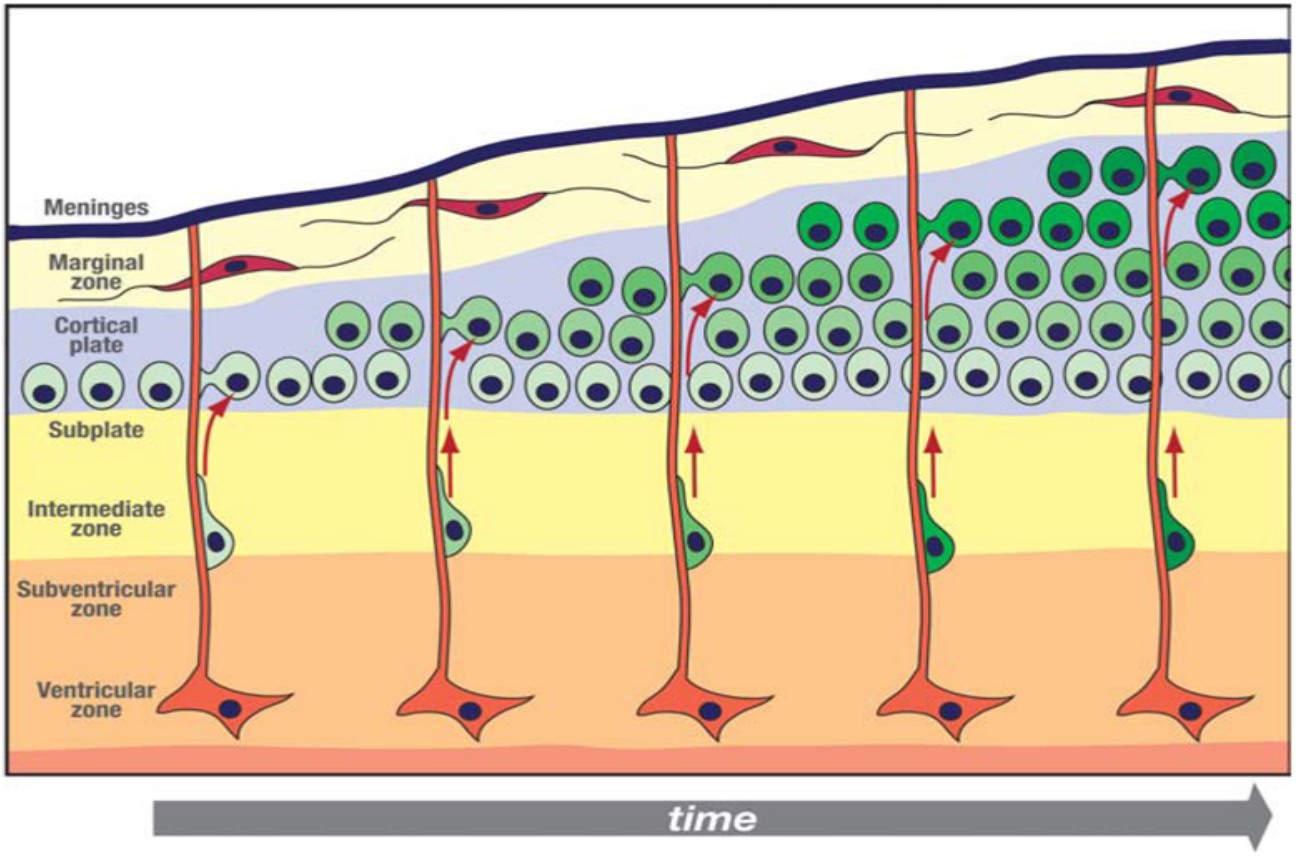


**Figure 1** Schematic diagram of radial-directed cortical neuronal migration. Neurons (*green*) are generated in the ventricular zone and migrate along radial glial cells (*orange*) through the subventricular zone, intermediate zone, subplate, and cortical plate. The cortical plate is established in an inside-out pattern so that later-generated neurons (*progressively darker green shading*) destined for more superficial layers bypass earlier-generated neurons in deeper layers. The marginal zone includes horizontally oriented Cajal-Retzius (*red*). The most superficial cortical structure is the pia/meninges.

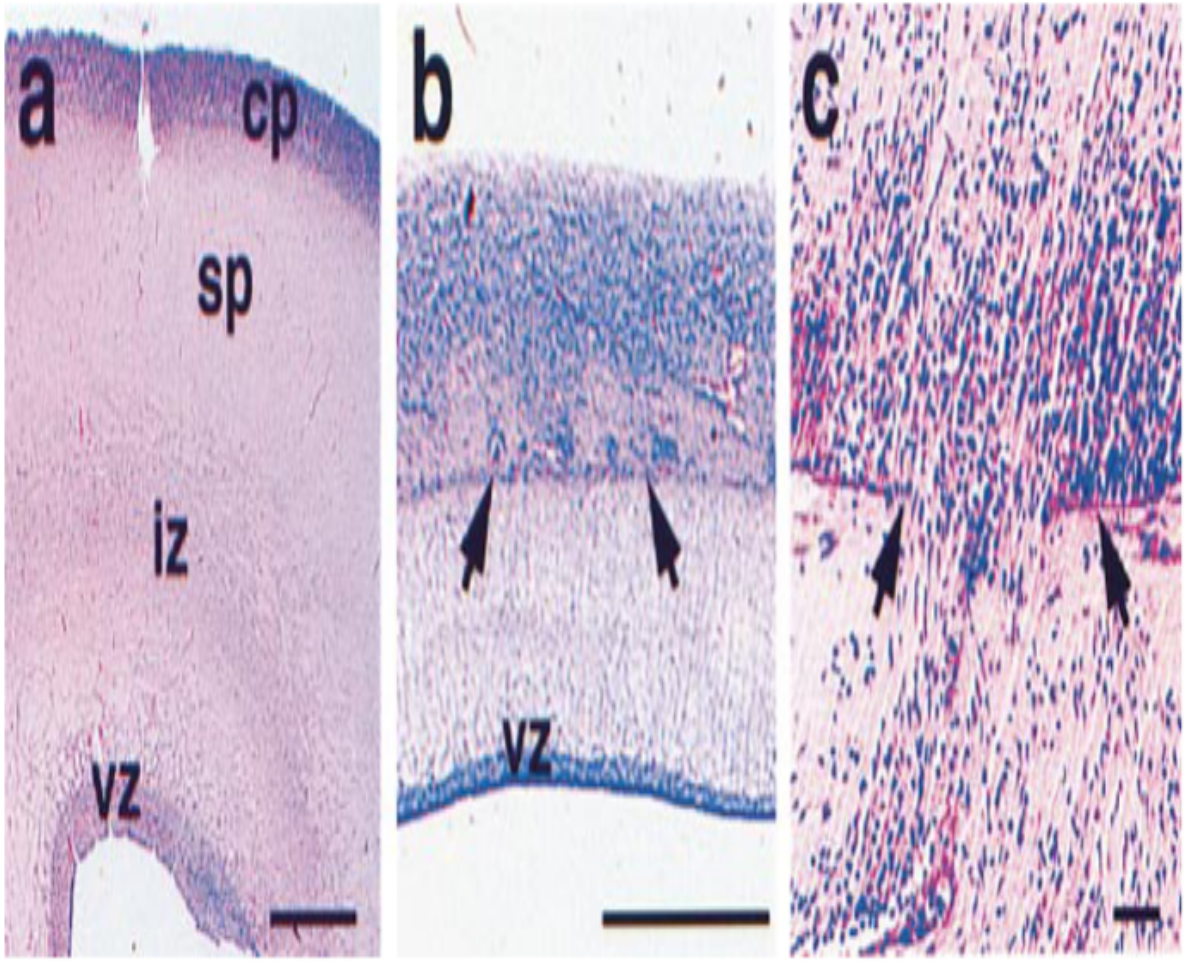


Figure 4. Cellular Appearance of Cobblestone (Type II) Lissencephaly

The photomicrographs contrast (a) a normal human fetal brain (22 weeks gestation) with the brain of a fetus of the same age with cobblestone lissencephaly due to Walker-Warburg syndrome (b and c). The brain in cobblestone lissencephaly (b) is less than half of normal thickness and lacks the clear stratification of the ventricular zone (vz), intermediate zone (iz), subplate (sp), and cortical plate (cp) seen in the normal brain (a). In both pictures, the ventricular surface is down and the pial surface is up. In (b), the location of the normal pial surface is indicated by arrows. The dark blue nuclei represent migrating cells that have penetrated the pia and flowed out randomly over the outer surface of the pia. The photomicrograph in (c) shows a higher power view of one of the defects in the pia, with immature neuroblasts migrating through it. Scale bar in (a) and (b), 1 mm; in (c), 100 μm.

# Muscle Eye Brain Disease (MEB)

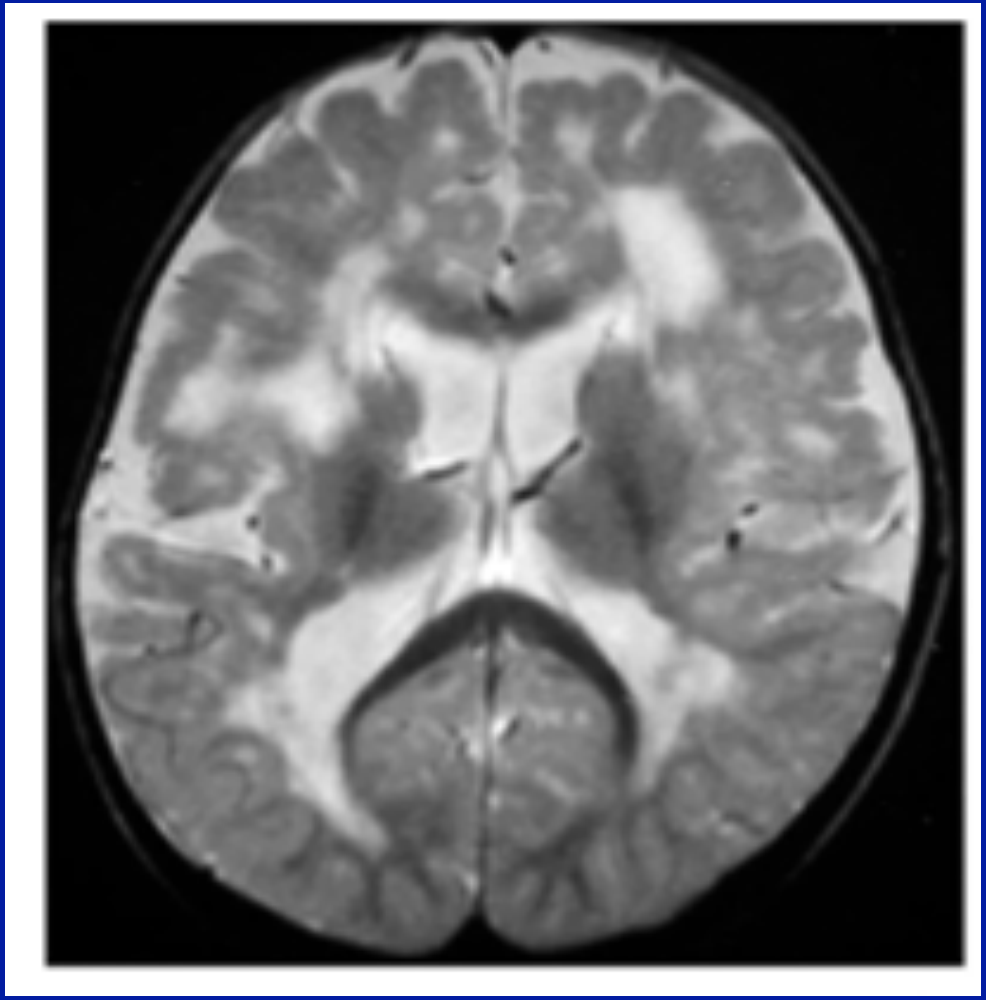

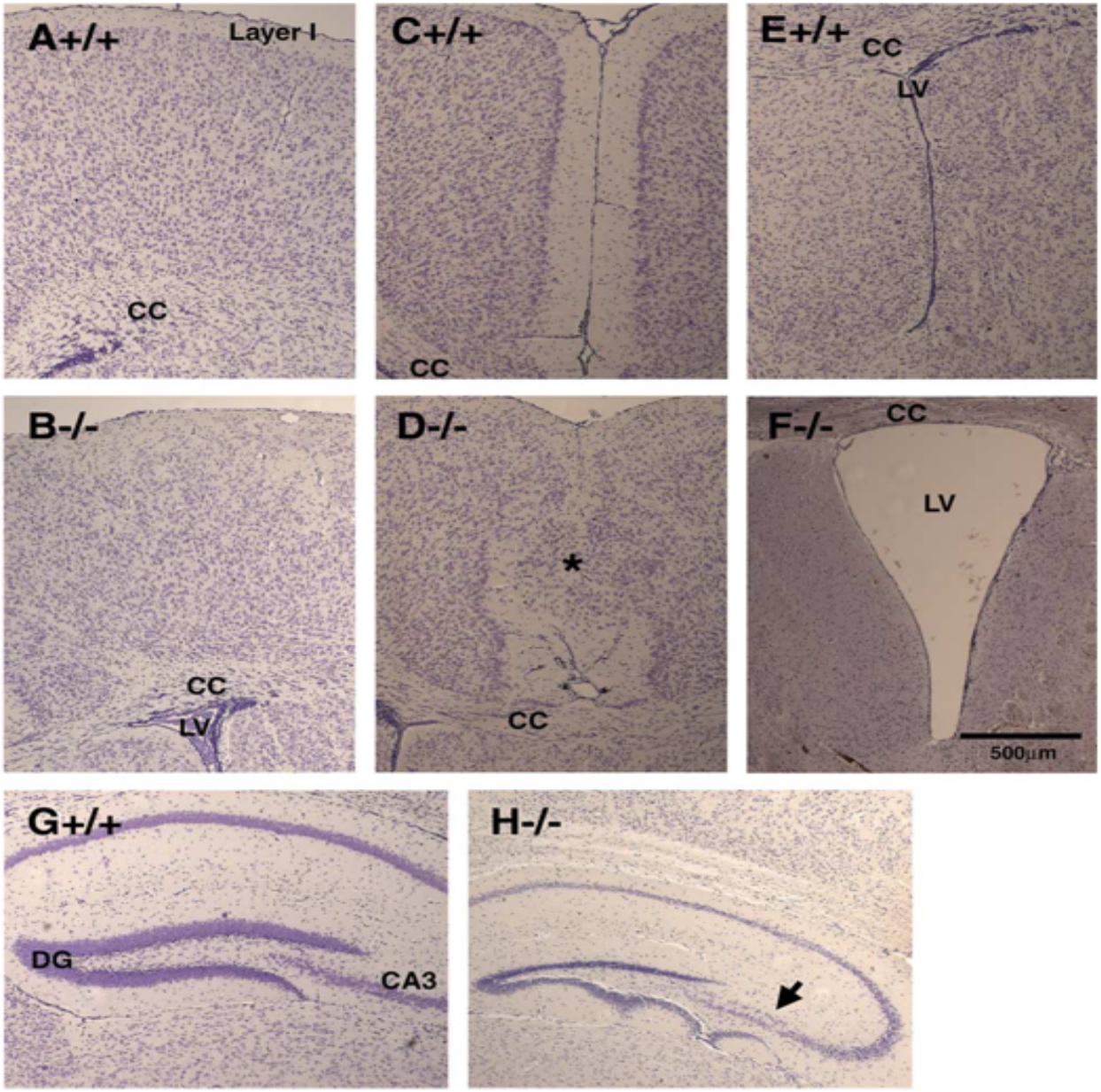


Fig. 6. Multiple abnormalities in the forebrain of POMGnT1 mutant mice. Paraffin sections of the forebrain were Nissle-stained (cresyl violet). (A) Wildtype cerebral cortex. (B) Mutant cerebral cortex. (C) Wildtype midline. (D) Mutant midline. (E) Wildtype lateral ventricle. (F) Mutant lateral ventricle. (G) Wildtype hippocampus. (H) Mutant hippocampus. Abbreviations: CC, caupus callosum; DG, dentate gyrus; LV, lateral ventricle. Scale bar in F, 500 μm.

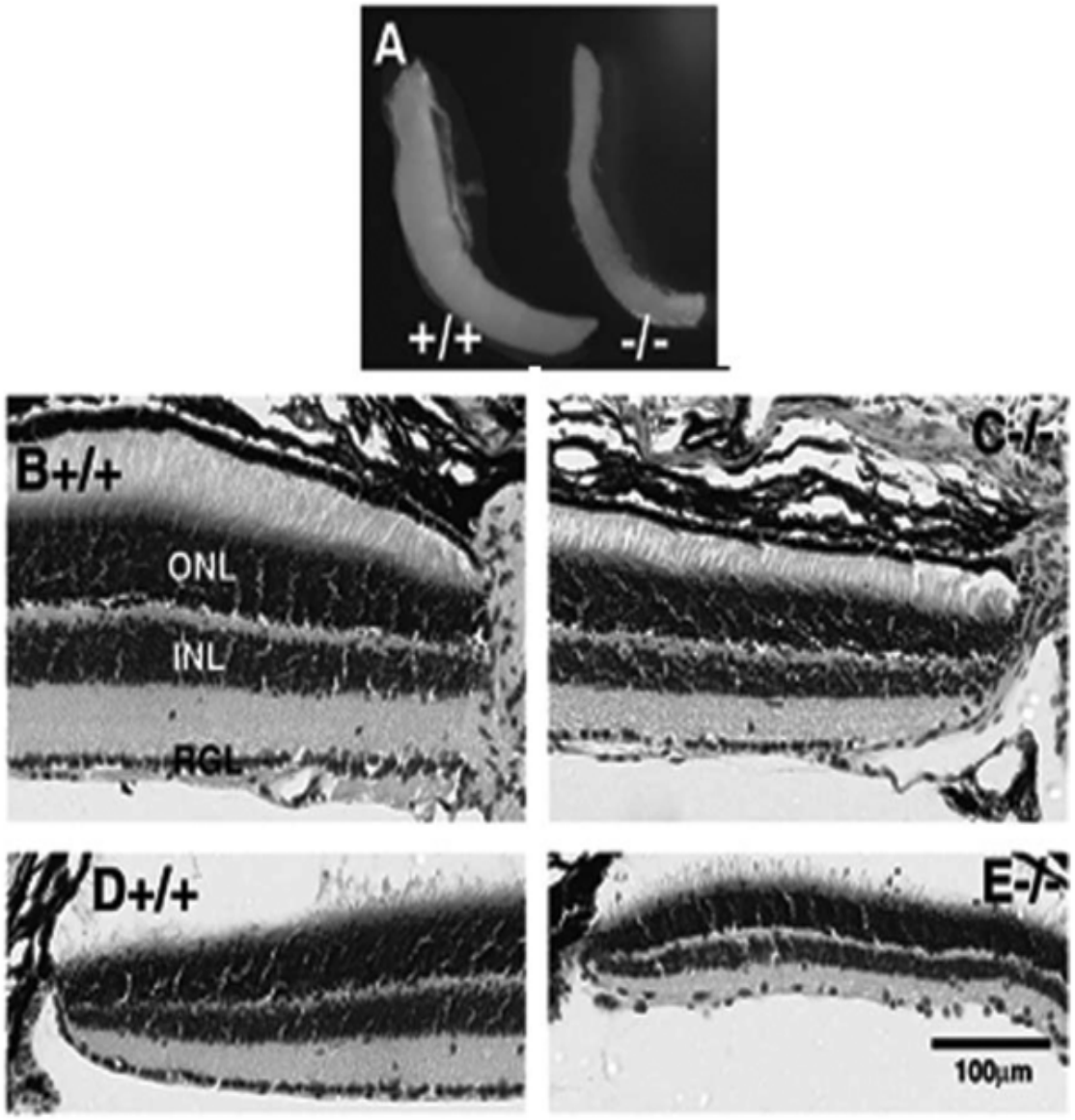


Fig. 7. Abnormal retina in POMGnT1 mutant mice. (A) Optic nerve of the mutant (−/−) and wildtype (+/+) mice. (B) Wildtype central retina. (C) Mutant central retina. (D) Wildtype peripheral retina. (E) Mutant peripheral retina. Note that the mutant retina has fewer ganglion cells especially in the peripheral retina. In addition, the retinal layers are thinner in the mutant. Abbreviations: INL, inner nuclear layer; ONL, outer nuclear layer; RGL, retinal ganglion cell layer. Scale bar in E, 100 μm for B–E.

# Limb Girdle Muscular Dystrophy 2I

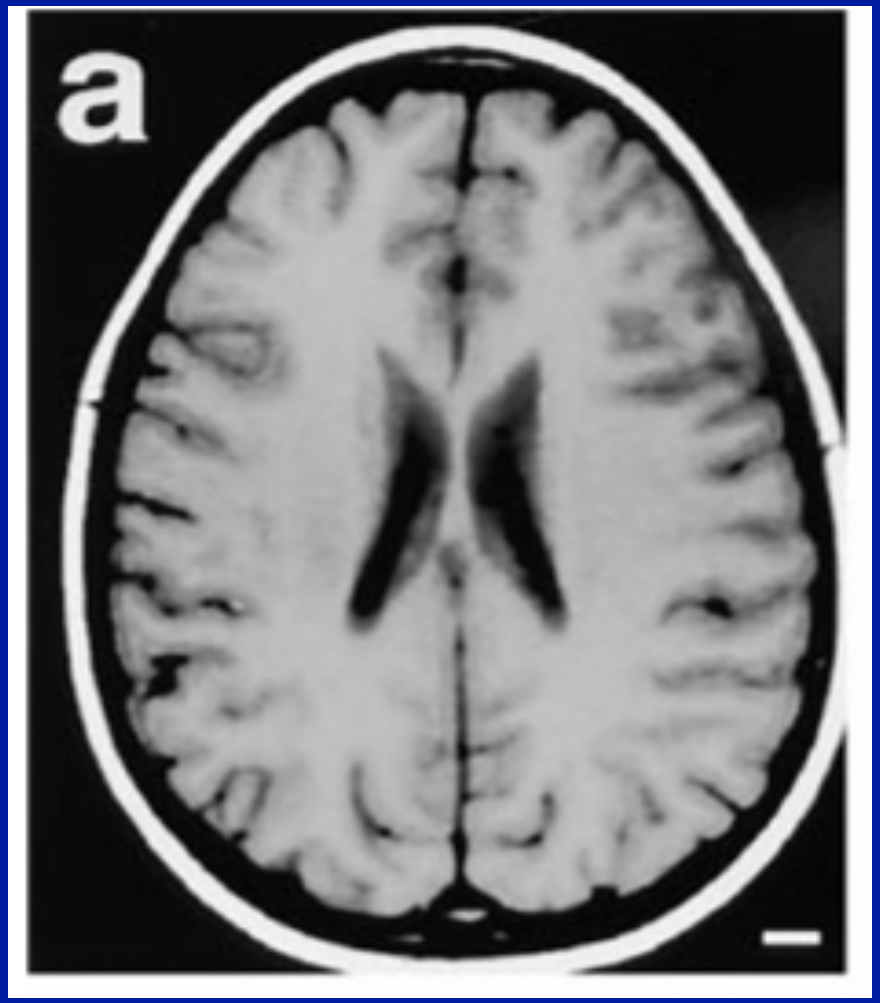

# Still undefined dystroglycanopathy mutations

Vuillaumier-Barrot et al. 2012
*Am J. Hum. Genet.*
**91**, 1135

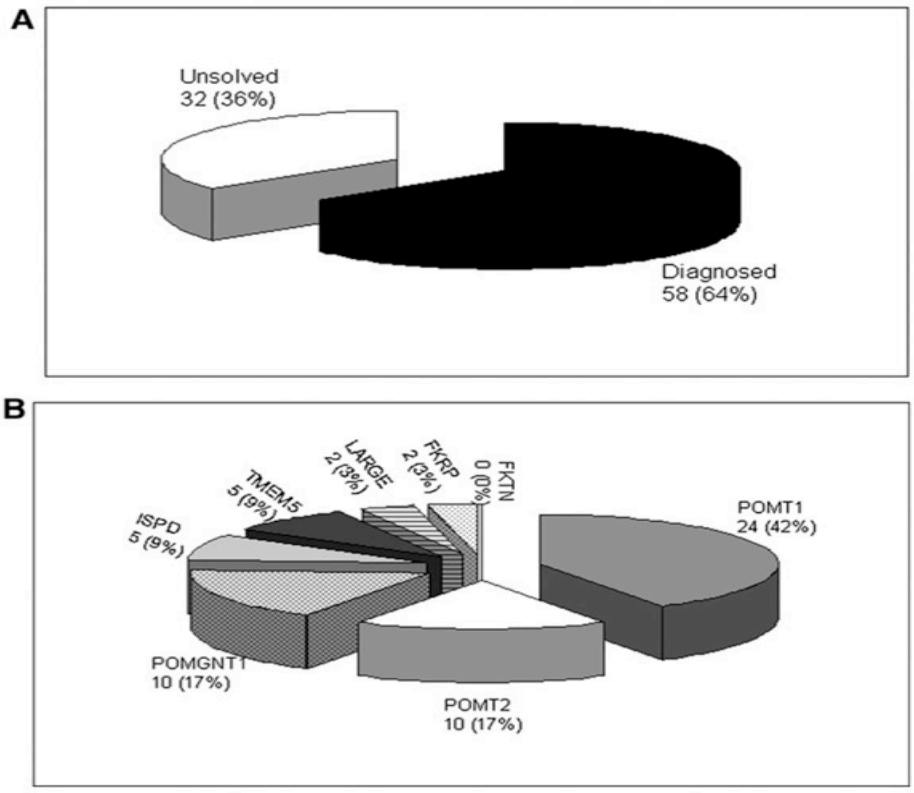


**Figure 2. Results of Molecular Diagnosis of Cobblestone-LIS Fetuses**
(A) Proportion of cases diagnosed after this study in our cohort of 90 cobblestone-LIS fetuses.
(B) Contribution of alpha-dystroglycanopathy gene mutations in our 58 diagnosed cobblestone-LIS fetuses.

# Using patient-derived fibroblasts to define new disease mutations by gene rescue

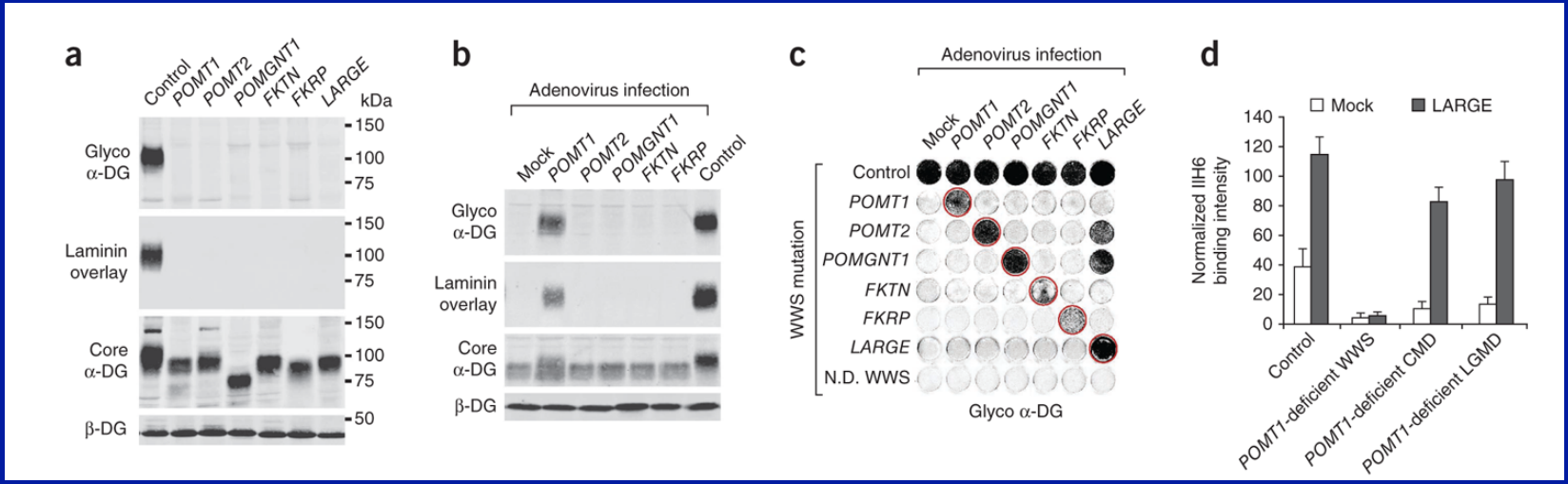


Willer et al. (2012) *Nature Genetics* **44**, 575-80

# Fibroblast fusion genetic complementation assay defines five new disease genes

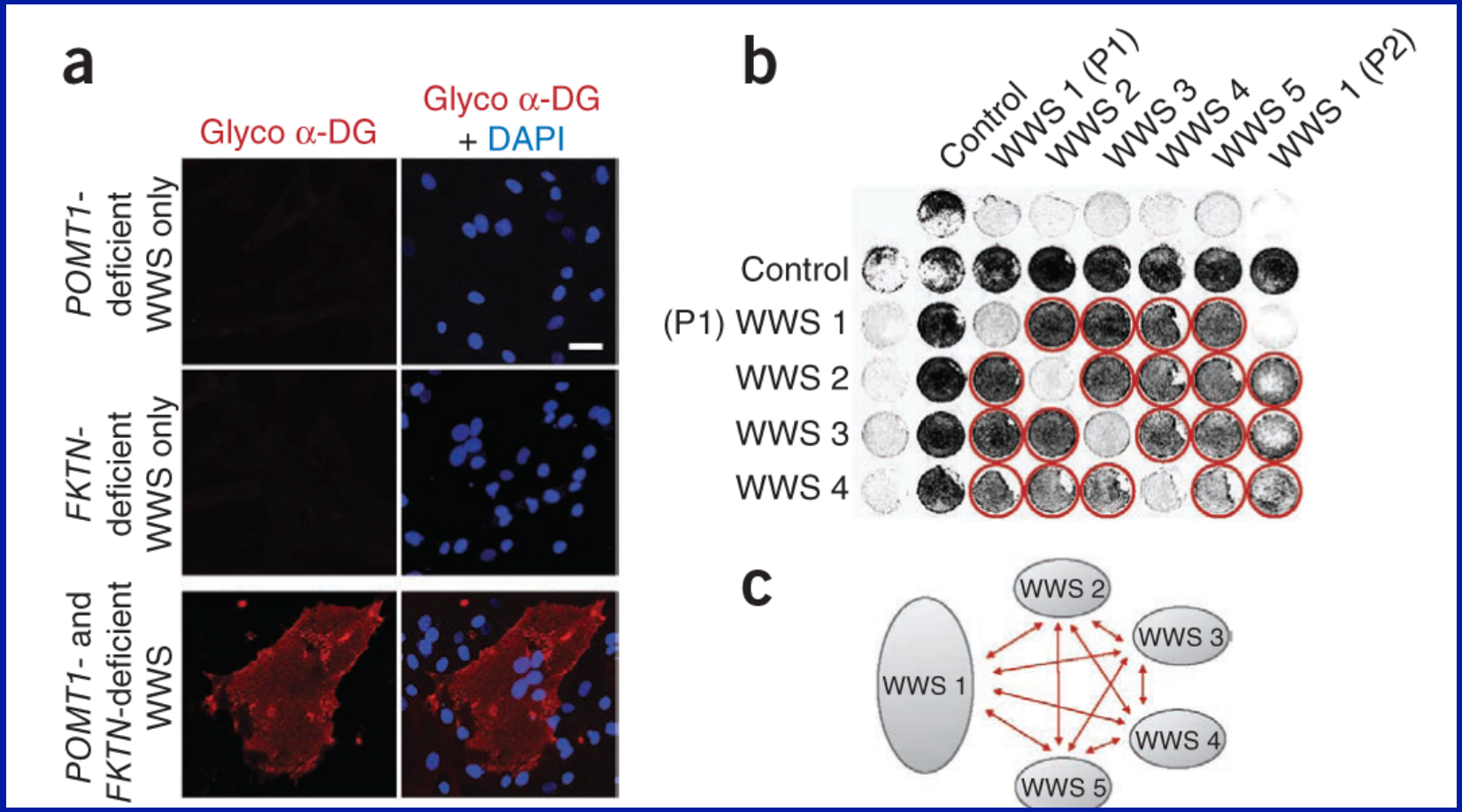

# Targets for Therapy in Dystroglycanopathies

Gene Replacement (FKRP, Fukutin, Large)

Overexpression of glycosyltransferases

Large, Large2, B3GnT1

Inhibit protein misfolding, localization or degradation. FKRP,Fukutin

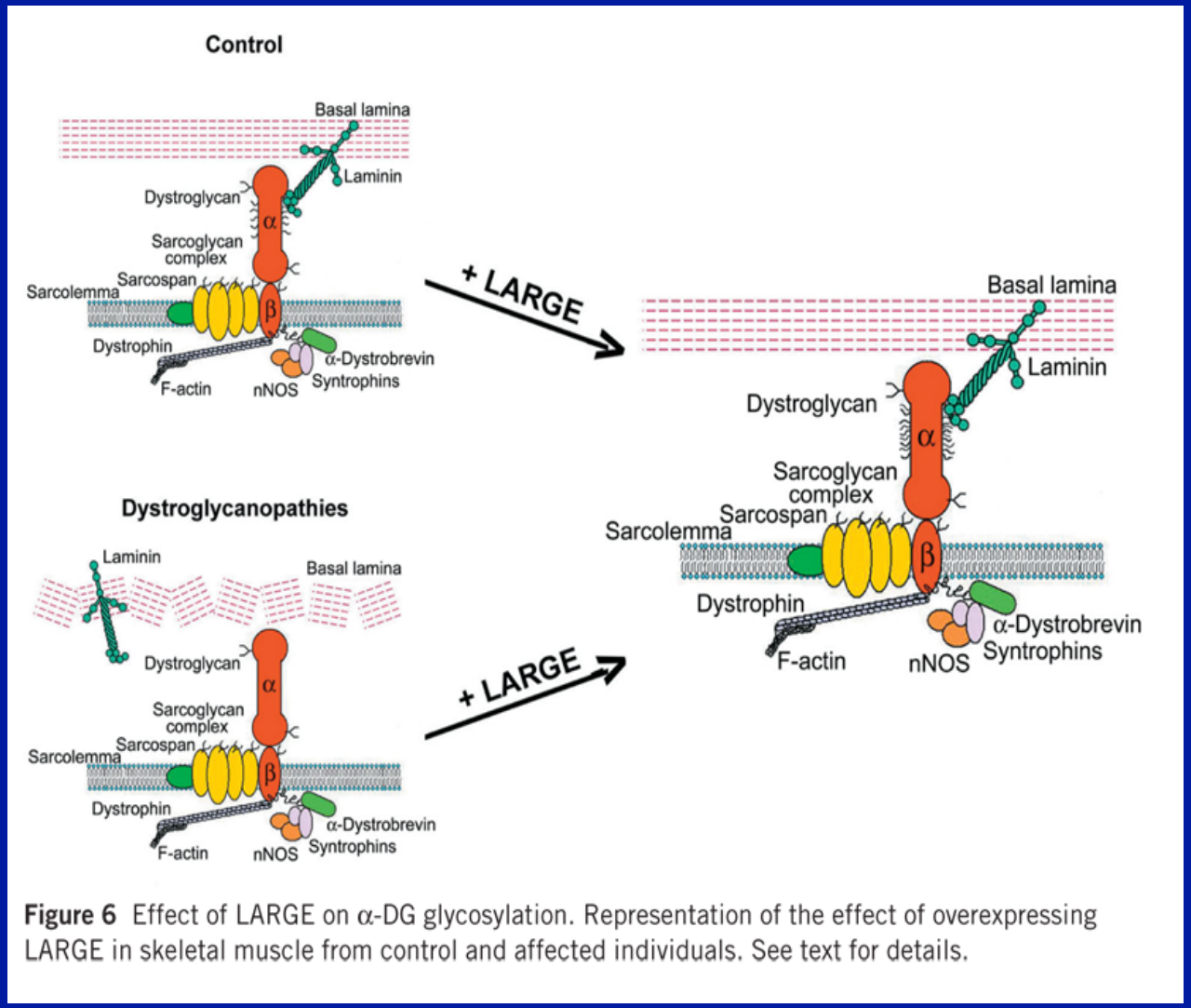


**Figure 6** Effect of LARGE on α-DG glycosylation. Representation of the effect of overexpressing LARGE in skeletal muscle from control and affected individuals. See text for details.

Baressi et al 2004 *Nature Med.* **10**, 696

# LARGE overexpression in FCMD patient myoblasts reglycosylates αDG and yields functional laminin binding

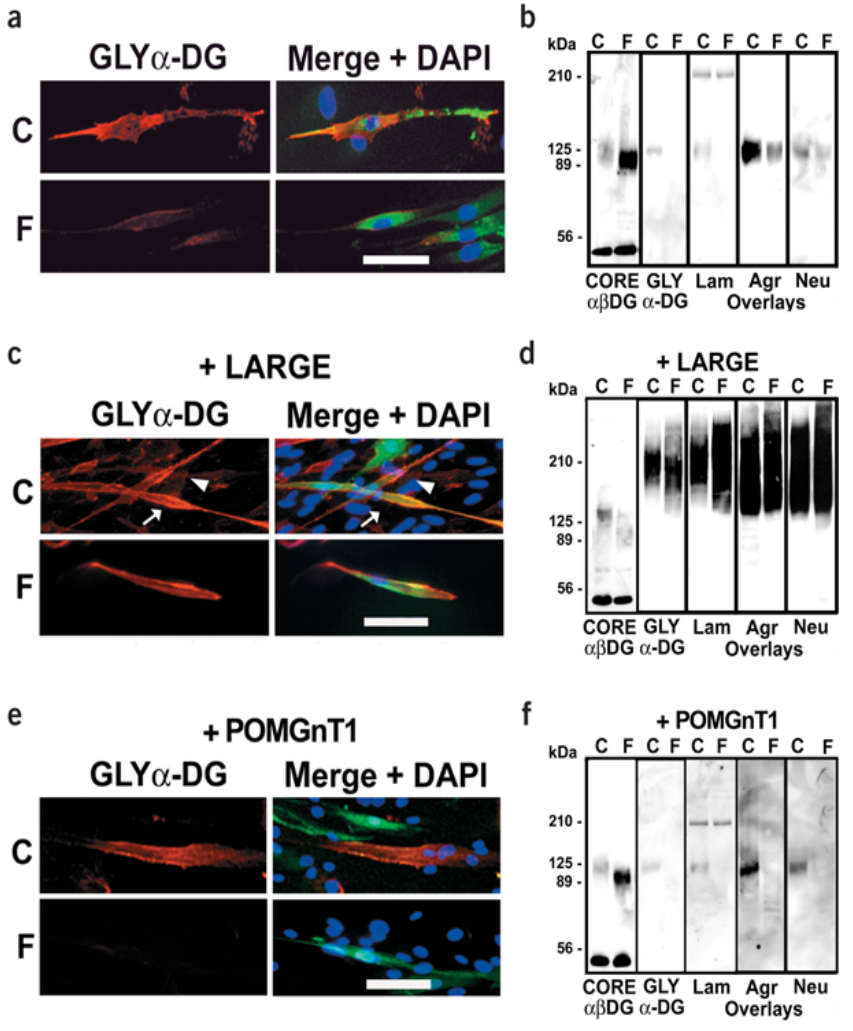


**Figure 2** LARGE generates functional α-DG in FCMD myoblasts. (**a**–**f**) Analysis of untreated (**a**,**b**), or infected with Ad5-LARGE-eGFP (**c**,**d**) or Ad5-POMGnT1-eGFP (**e**,**f**) control (C) and FCMD (F) cultures. Immunofluorescence shows localization of desmin (**a**) or eGFP (**c**,**e**). Arrows indicate myotubes and arrowheads indicate myoblasts. Scale bars, 10 μm. WGA-enriched lysates of treated cultures were also analyzed by SDS-PAGE followed by immunoblot analysis with antibodies to DG core protein (CORE-αβDG) and glycosylated α-DG (**b**,**d**,**f**). Laminin (Lam), neurexin (Neu) and agrin (Agr) were used for ligand overlay assays. Bands at ~210 kDa in **b** and **f** are endogenous laminin. Data are representative of three individuals with FCMD.

Baressi et al 2004 *Nature Med.* **10**, 696

# LARGE overexpression in WWS patient myoblasts reglycosylates αDG and yields functional laminin binding

Baressi et al 2004 *Nature Med.* **10**, 696

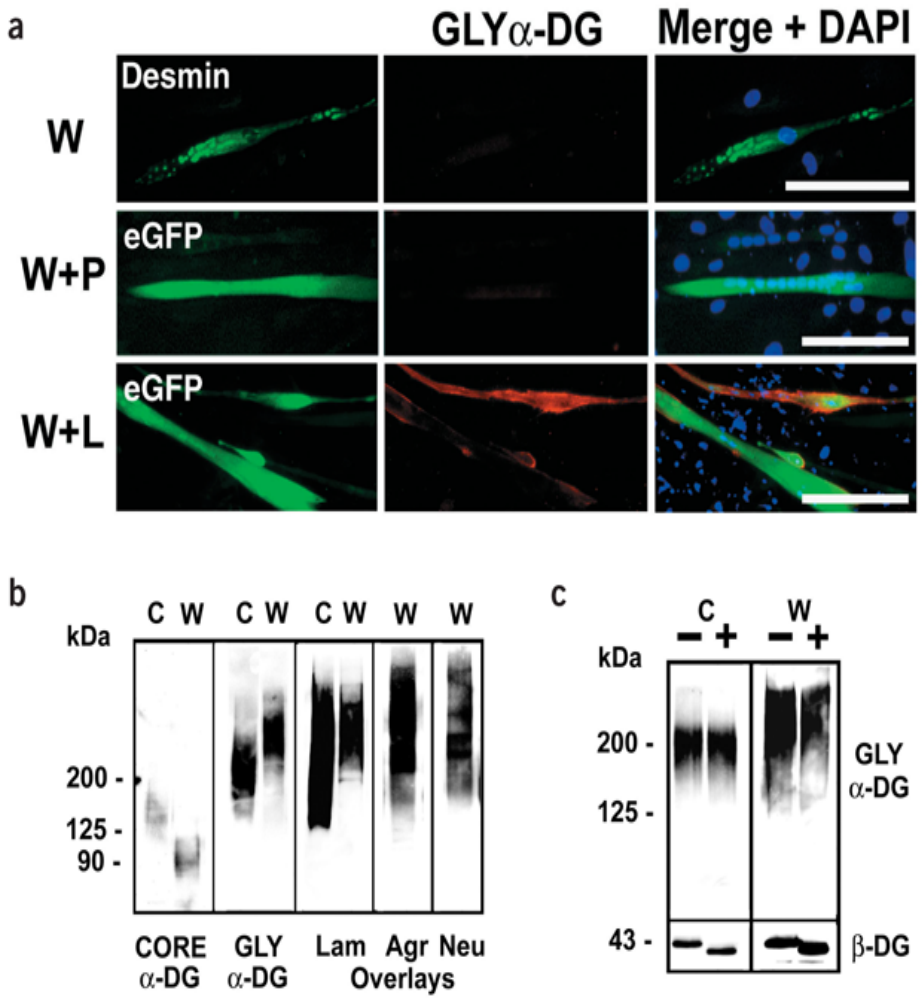


**Figure 4** LARGE induces the synthesis of functional α-DG in WWS myoblasts and myotubes. (**a**) Expression of eGFP, desmin (green, upper row) and glycosylated α-DG (GLYα-DG), and nuclear labeling (DAPI, blue) in WWS myoblasts either untreated (W) or treated with Ad5-LARGE-eGFP (W+L) or Ad5-POMGnT1-eGFP (W+P). Scale bar, 20 μm. (**b**) Biochemical analysis of WGA-enriched fractions from control (C) and WWS myoblasts (W) treated with Ad5-LARGE-eGFP. Immunoblotting was done with antibodies to glycosylated α-DG and α-DG core protein (COREα-DG). Ligand overlay assays were done for laminin (Lam), agrin (Agr) and neurexin (Neu). (**c**) *N*-glycanase deglycosylation of WGA-enriched fractions from control (C) and WWS myoblasts (W) treated with Ad5-LARGE-eGFP. Immunoblotting was done with antibodies to β-DG and glycosylated α-DG. Untreated samples (–) are shown. Data are representative of four individuals with WWS.

# LARGE Tg mice show increased glycosylation as per IIH6 blot, but lower specific force

## Brockington et al. (2010) *PLOS ONE,* 5, e14434

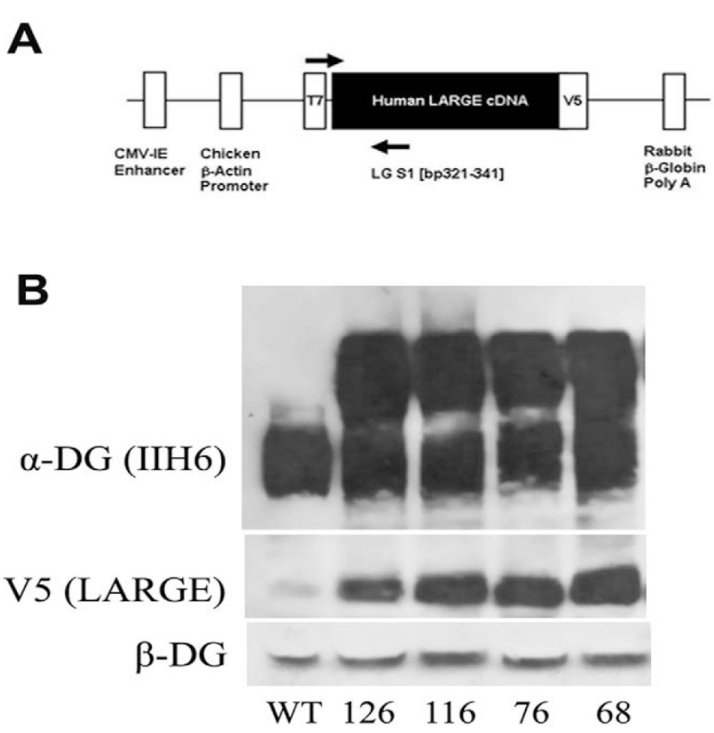


**Figure 1. Generation of LARGE transgenic mouse. A**. A schematic representation of the LARGE expression cassette. The full-length V5 tagged LARGE cDNA was subcloned into the pCAGGS expression vector. This vector consists of a synthetic CMVenhancer/and chicken β-actin promoter sequence located upstream of the transgene and the rabbit β-globin poly(A) sequence located downstream. Arrows represent position and orientation of PCR primers used to screen ear biopsies. **B**. Western blotting analysis of protein lysates from wild type and muscle tissues (quadriceps) from all the four LARGE transgenic lines (68,76,116 and 126) using antibodies to α-DG IIH6, β-DG, and V5.
doi:10.1371/journal.pone.0014434.g001

# LARGE Tg increases high MW laminin binding in skeletal muscle and heart, but not brain

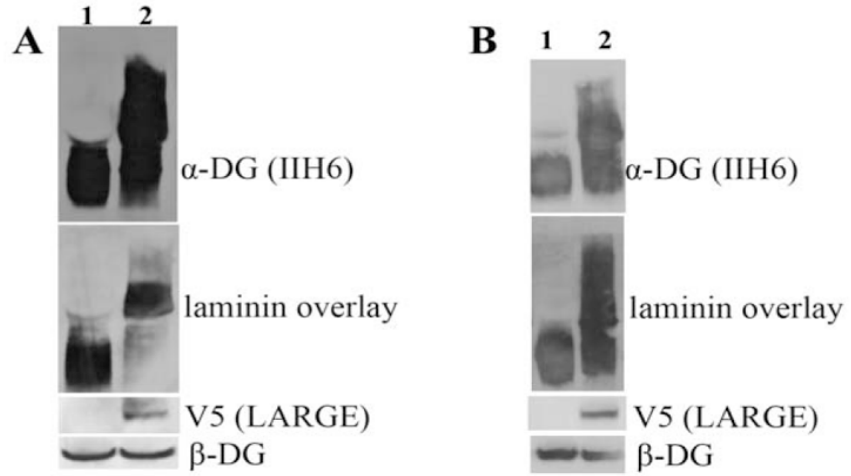


**Figure 3. Western blot and laminin assay analysis of LARGE transgenic mouse tissues.** Western blot analysis of protein lysates from wild type and LARGE transgenic (line 68) tissues using antibodies to α-DG IIH6, β-DG, and V5. **A**. Wild type and LARGE transgenic *quadriceps* muscle. When the membrane was exposed for a short period using antibody IIH6 a clear band of higher molecular weight was detected in the samples from LARGE transgenic muscle compared to controls, while a longer exposure resulted in a continuous smear. Laminin-1 overlay showed that hyperglycosylated α-DG has increased laminin binding. β-DG expression was unaltered in transgenic mice. **B**. Wild type and LARGE transgenic mouse cardiac muscle. Laminin-1 overlay showed that hyperglycosylated α-DG bound laminin with a similar capacity to normally glycosylated dystroglycan.

# LARGE overexpression increases muscle pathology in FKRP mutant mice (Whitmore et al. (2013) *Hum. Mol. Genet.*In Press *)*

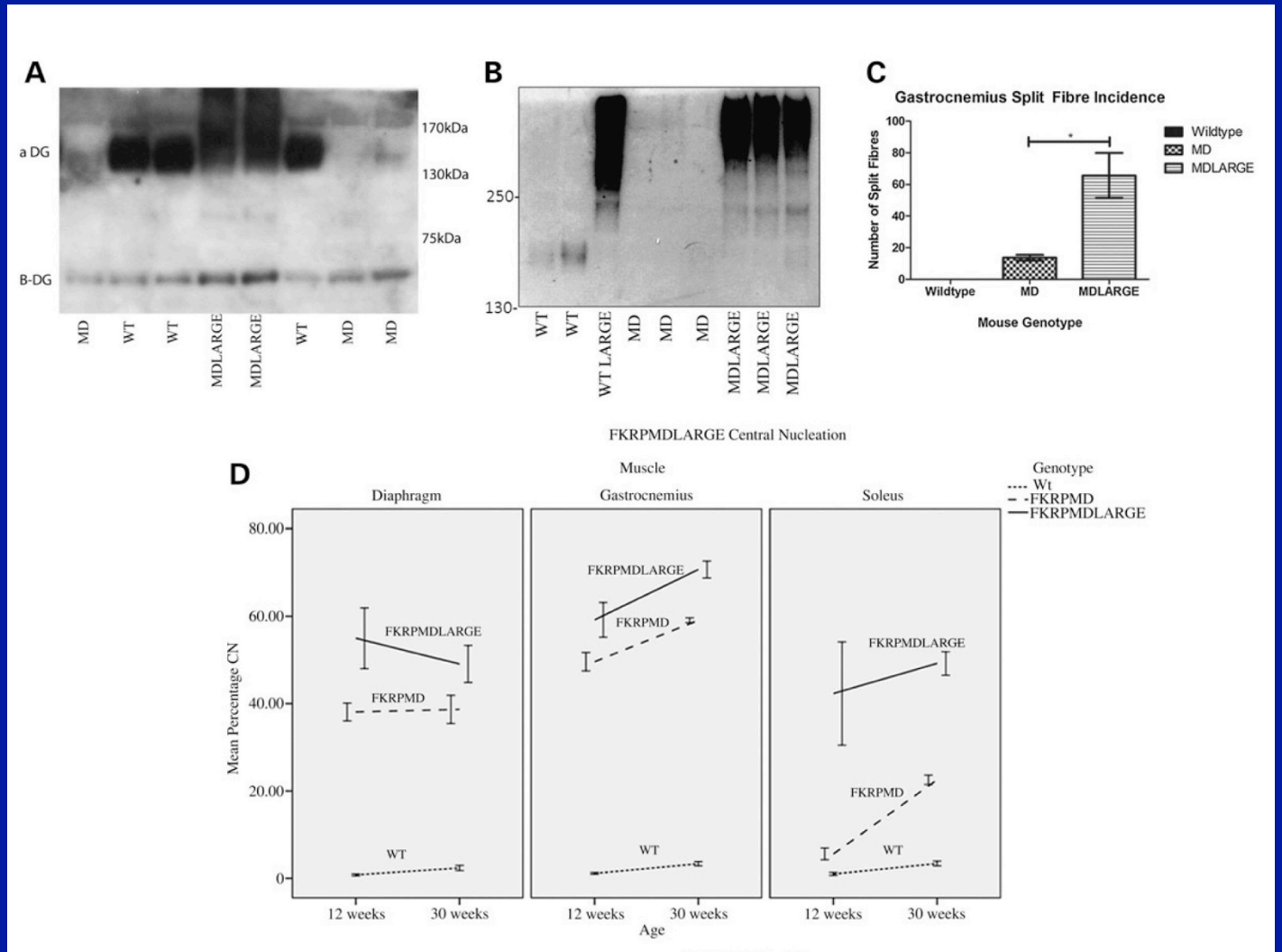

# LARGE overexpression increases loss of muscle strength in FKRP mutant mice

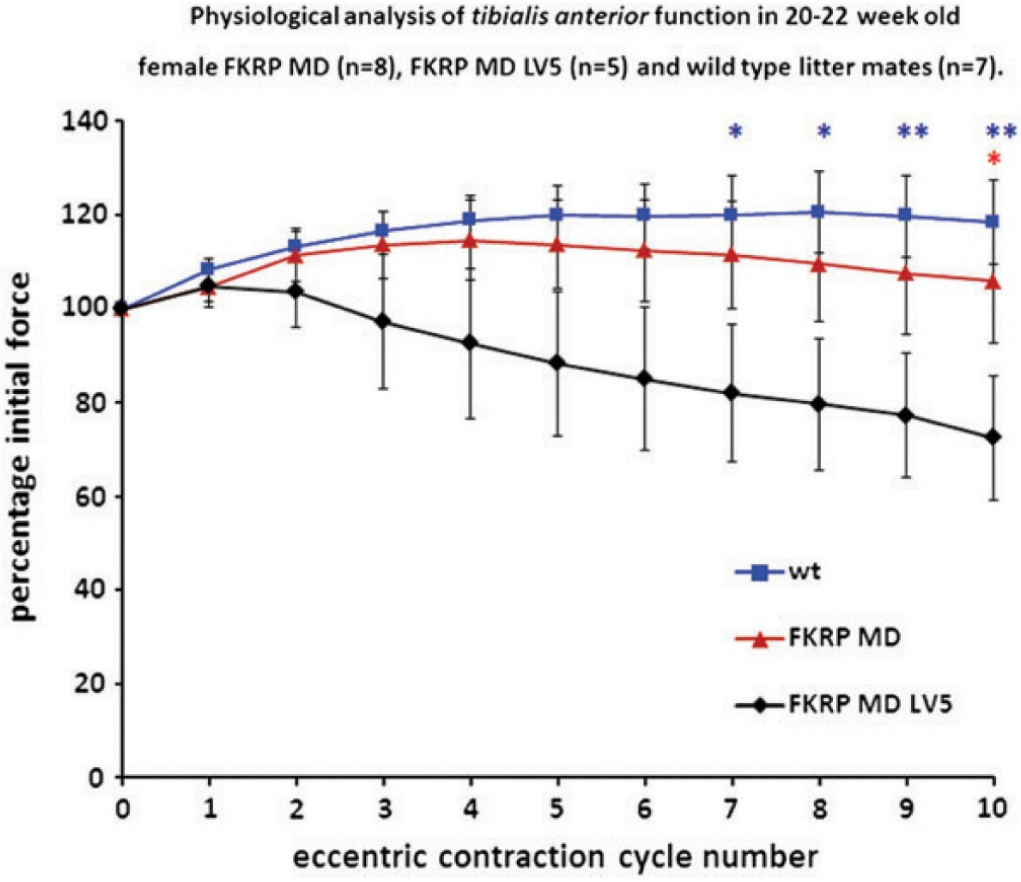


**Figure 8.** *In vivo* assessment of muscle force production following eccentric contractions. Tibialis anterior muscles from 20- to 22-week-old female $FKRP_{MD}$

# Dystroglycanopathies Congenital and Limb Girdle Muscular Dystrophies

Genes
*B3GNT1*

Potential disaccharide poly (diLacNAc) synthase

Can co-IP with LARGE and can increase DG glycosylation in cancer cells

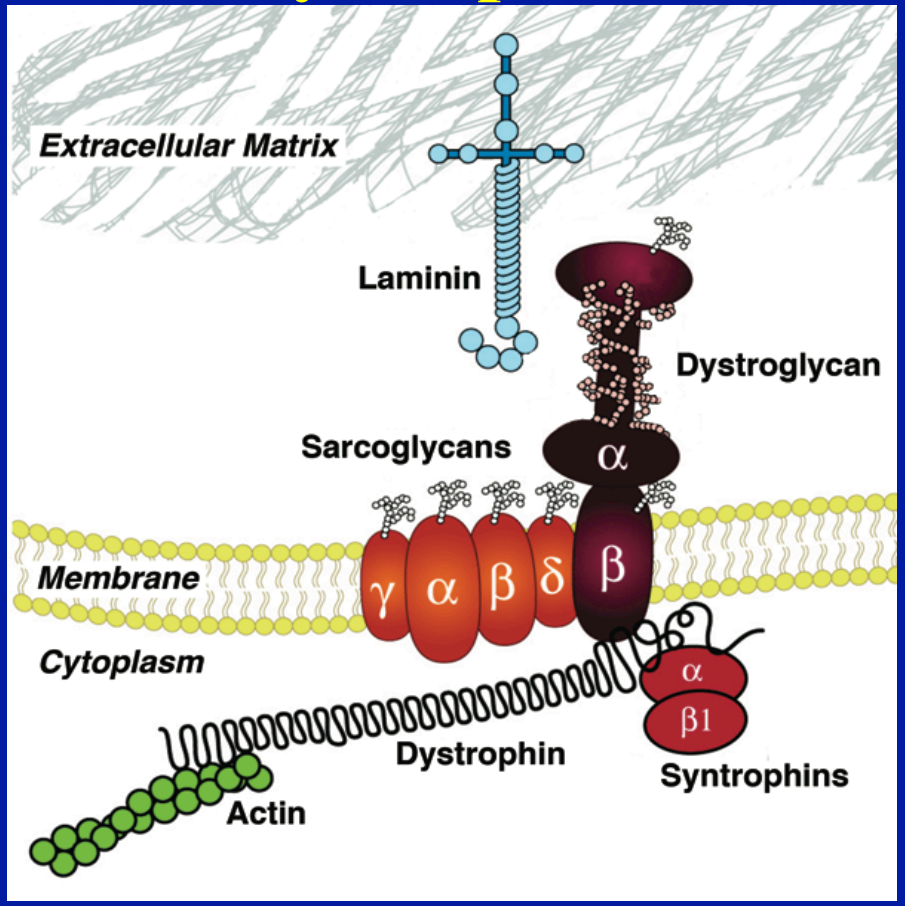


GlcNAcβ1,3Galβ1,4GlcNAcβ1,3Galβ1,4-

# b3GnT1 increases IIH6 in prostate cancer cells

**Bao et al. (2009) *PNAS* 29, 12109**

Red-2nd
Blue-βDG
Green-IIH6

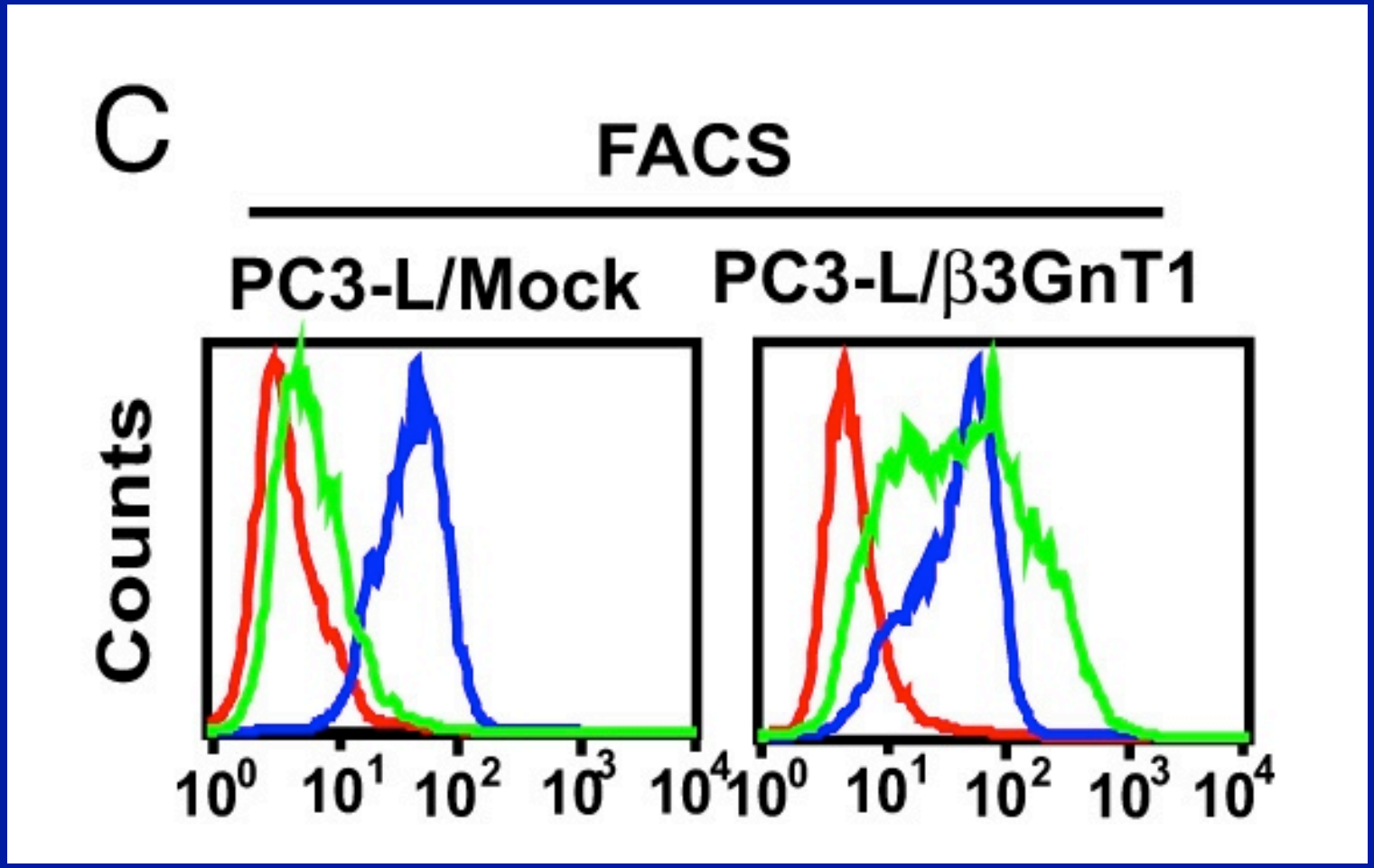

# b3GnT1 si RNAs decrease IIH6 in prostate cancer cells
# Bao et al. (2009 PNAS 29, 12109)

aDG
Largemyd
Control siRNA
b3GnT1 siRNA1
b3GnT1 siRNA2

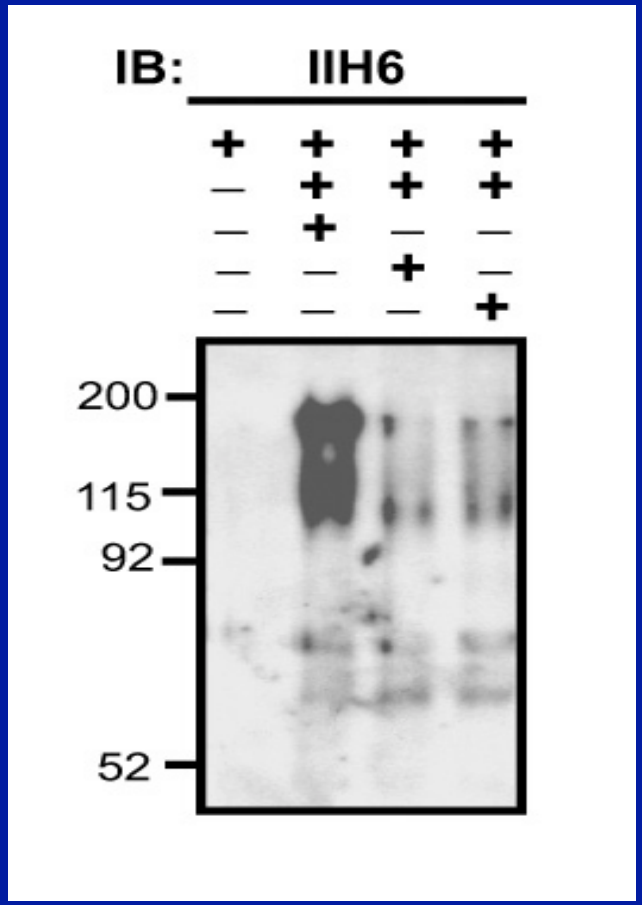

# Laminin G4-G5 Crystal structure, combined with mutagenesis data on ligand binding, suggests a long (6.5nm), charged (basic) and narrow binding pocket spanning both domains

LNα2 G4-G5
Domain structure
Tisi et al. 2000
*EMBO J*. 19(7), 1432

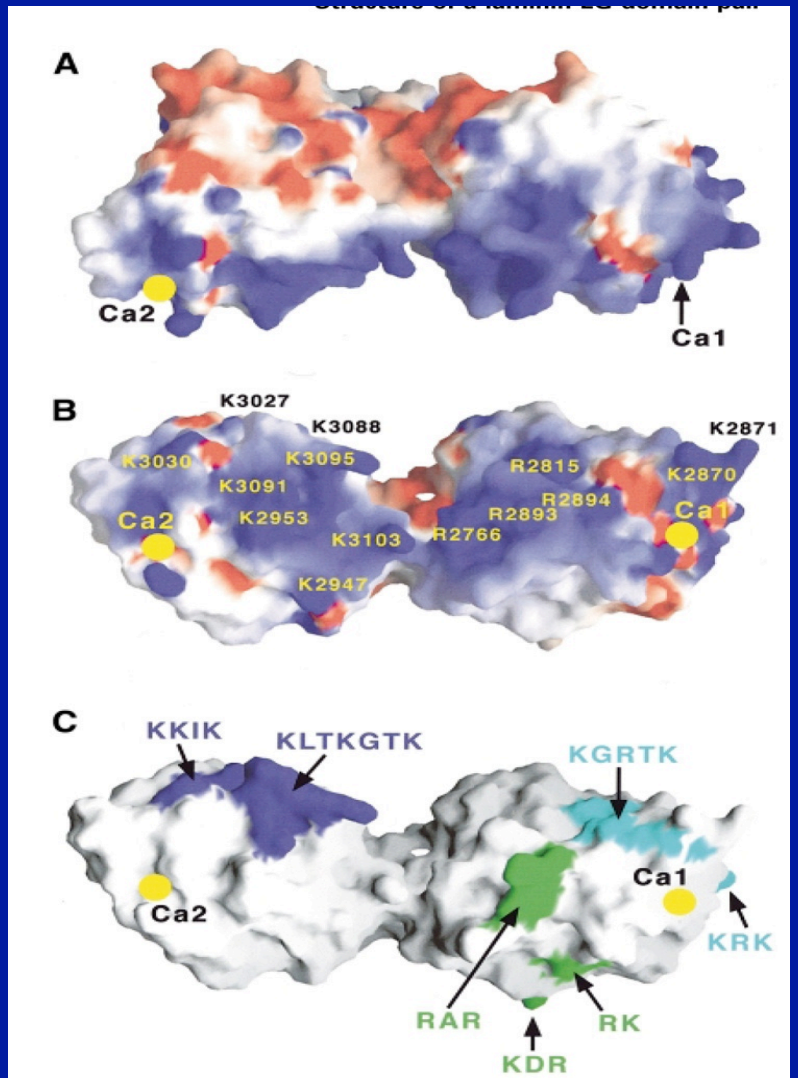

# Recent ideas about surrogate genes in CMDs

- HNK-1 ST – Inhibits LARGE glycosylation in CHO-K1 cells
- Fer Kinase – Downregulation increases expression of B3Gn3T1 and Large2 in prostate tumor cells
- Increase Galgt2 – Induce ectopic expression of synaptic DAG complex

# What puts on the breaks?
# Genes that may counterbalance CMD genes

**FucT3s** Galβ1,4**[Fucα1,3]**GlcNAcβ1,2Manα-O

**GnTIX/Vb** Neu5Ac/Gcα2,3Galβ1,4**GlcNAcβ1,6**Manα-O

**HNK-1 ST** **SO4-**GlcAβ1,3Galβ1,4GlcNAc

**O-GalNTs** Galβ1,3**GalNAcα**-O-Ser/Thr

LARGE GlcAβ1,3Xylα1,3GlcAβ1,3Xylα1,3

# HNK-1 Sulfotransferase overexpression inhibits LARGE activity CHO-K1 cell transfections

Nakagawa et al. (2013) *Glycobiology* **23**, 1066

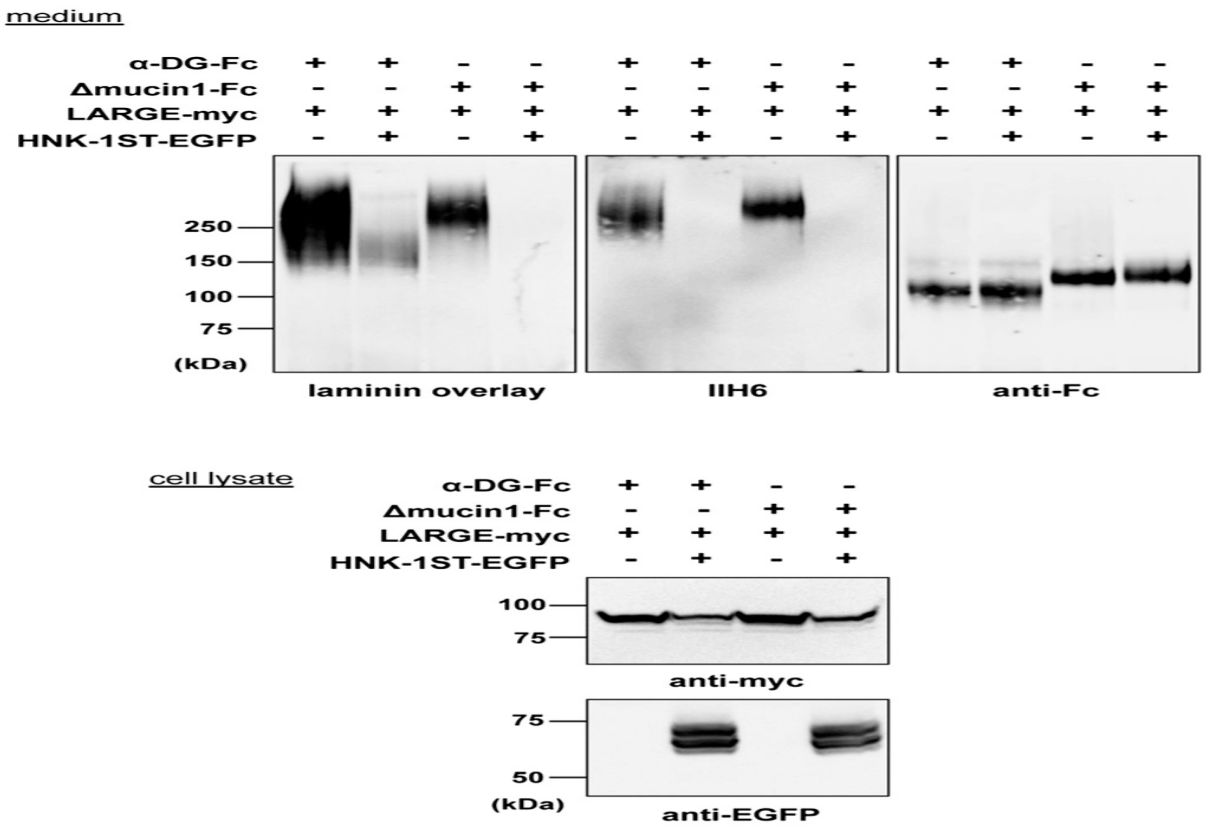


**Fig. 3.** Effect of HNK-1ST on Δmucin1-Fc with a single modification site for laminin-binding glycans. α-DG-Fc or Δmucin1-Fc and LARGE-myc were transiently coexpressed with or without HNK-1ST-EGFP as indicated. The secreted proteins were collected from the culture medium and analyzed by the laminin overlay assay and western blotting using IIH6 mAb and anti-Fc pAb

# Fer kinase affects Stat3 expression and b3GnT1, LARGE2 in prostate cancer cell DU145

Yoneyama et al 2012 *Mol. Biol. Cell* 23, 771

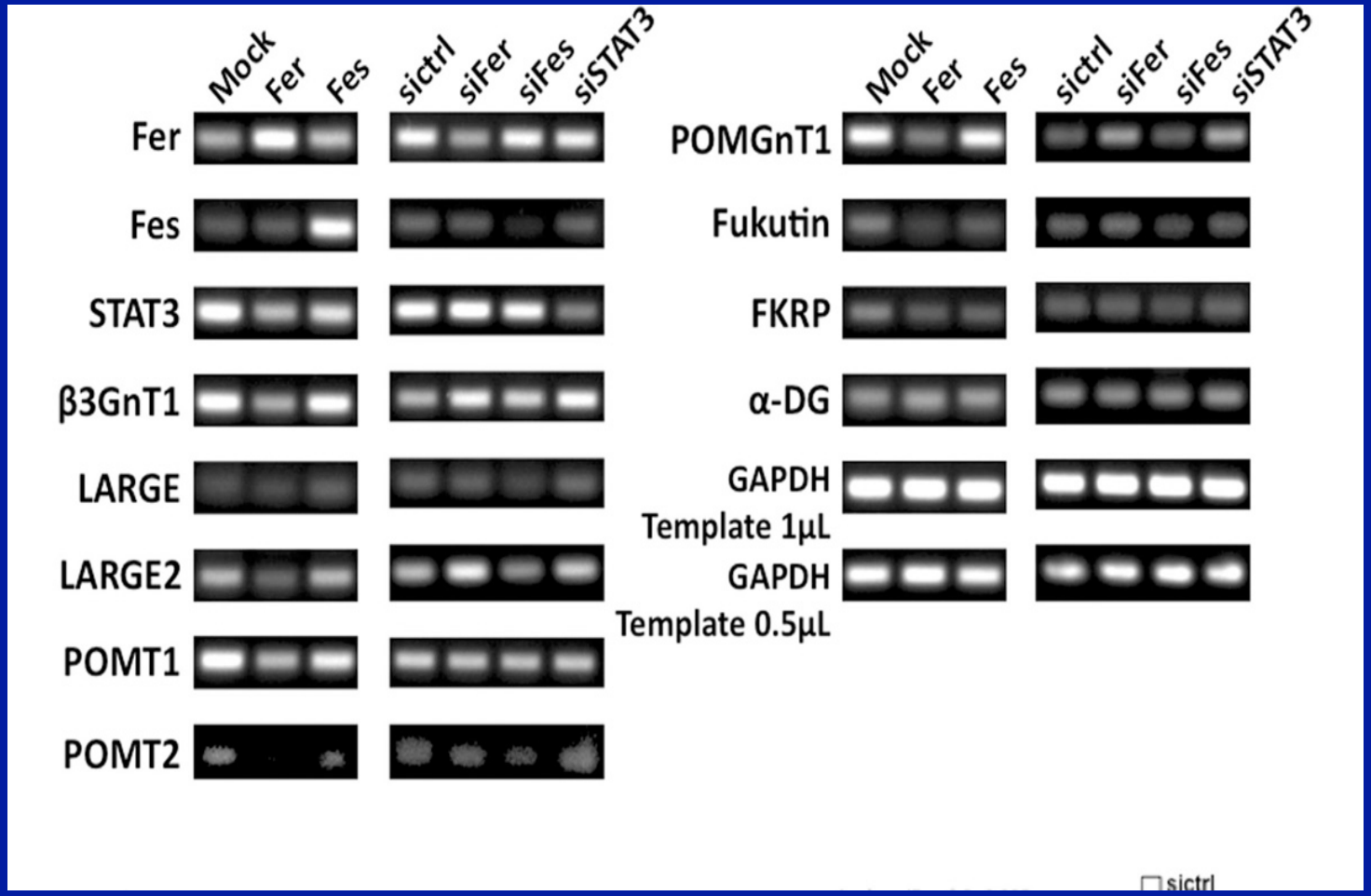

# The synaptic utrophin-associated glycoprotein complex

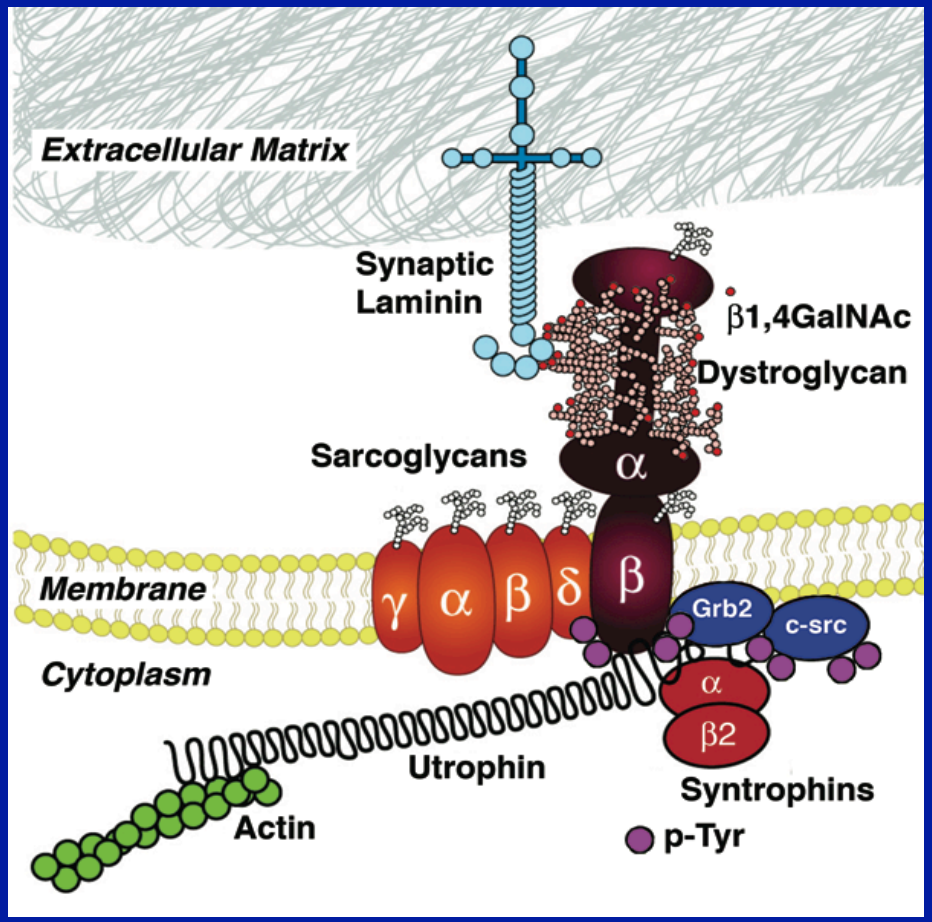


***B4GALNT2 (GALGT2)***

Neu5Ac/Gcα2,3**[GalNAcβ1,4]**Galβ1,4GlcNAcβ1,2Manα-O-Ser/Thr

# Galgt2 transgenic muscles overexpress synaptic αDG binding partners

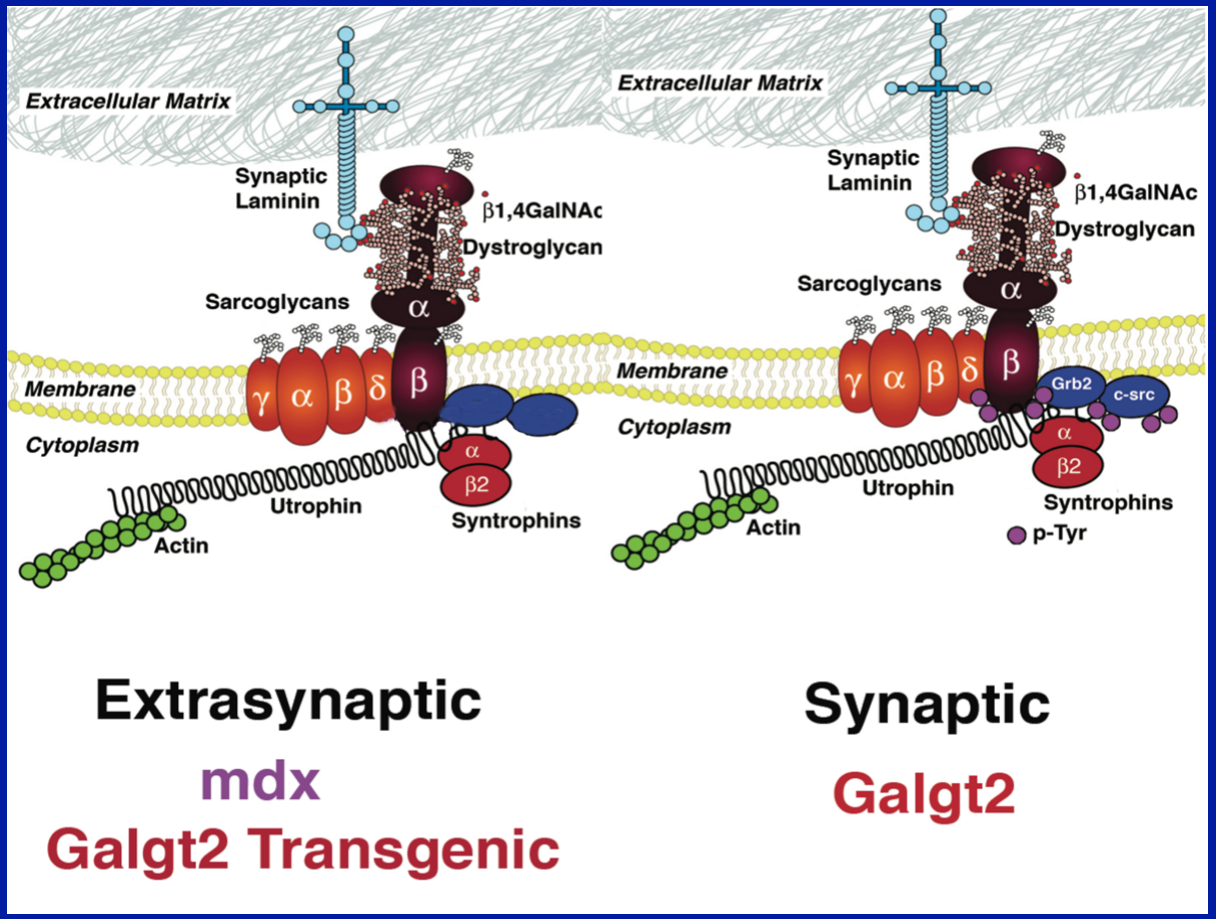

# Upregulation of the DAG complex at the sarcolemmal membrane

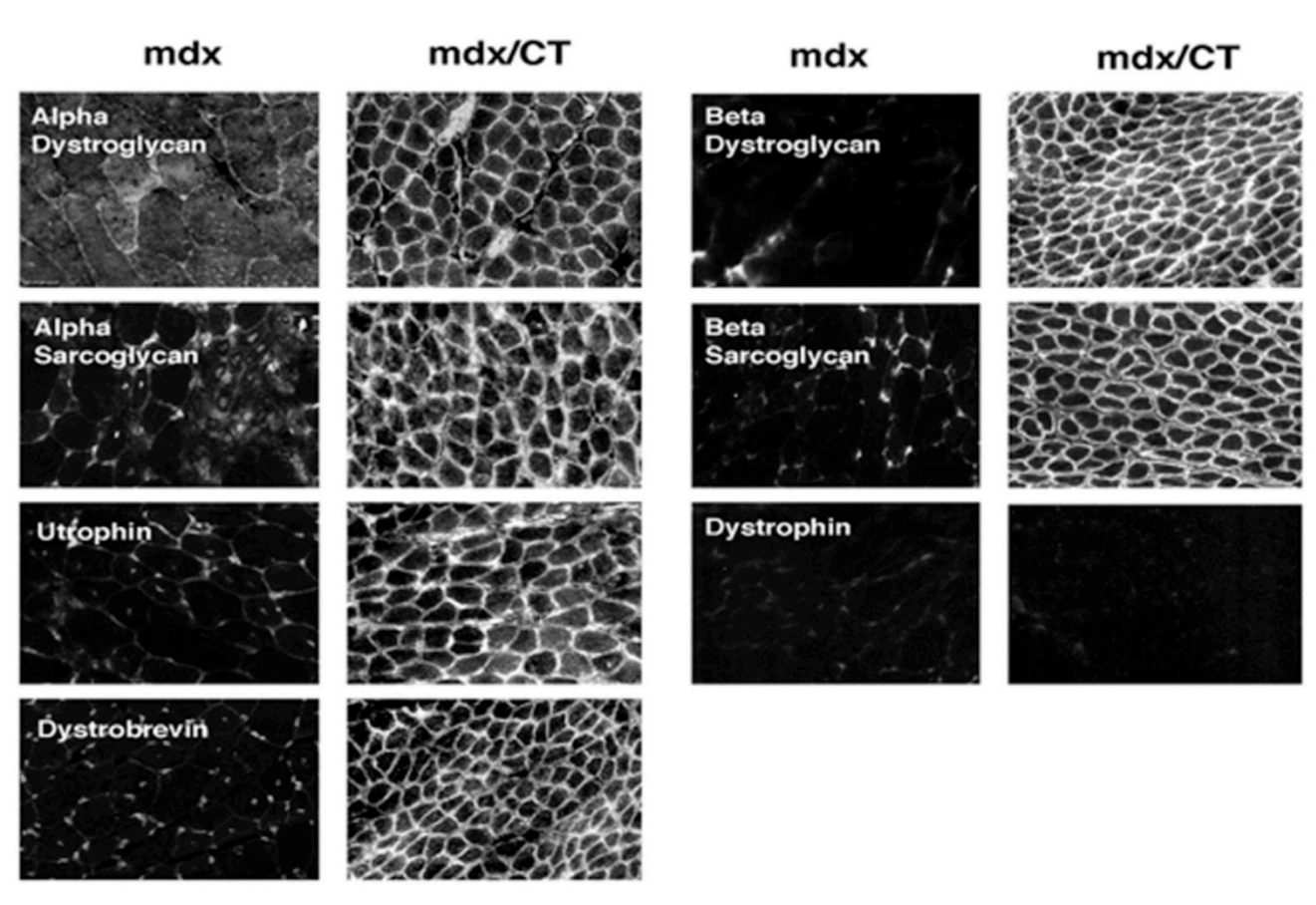

# Galgt2 (b4GalNt2) shows broad therapeutic potential in the muscular dystrophies

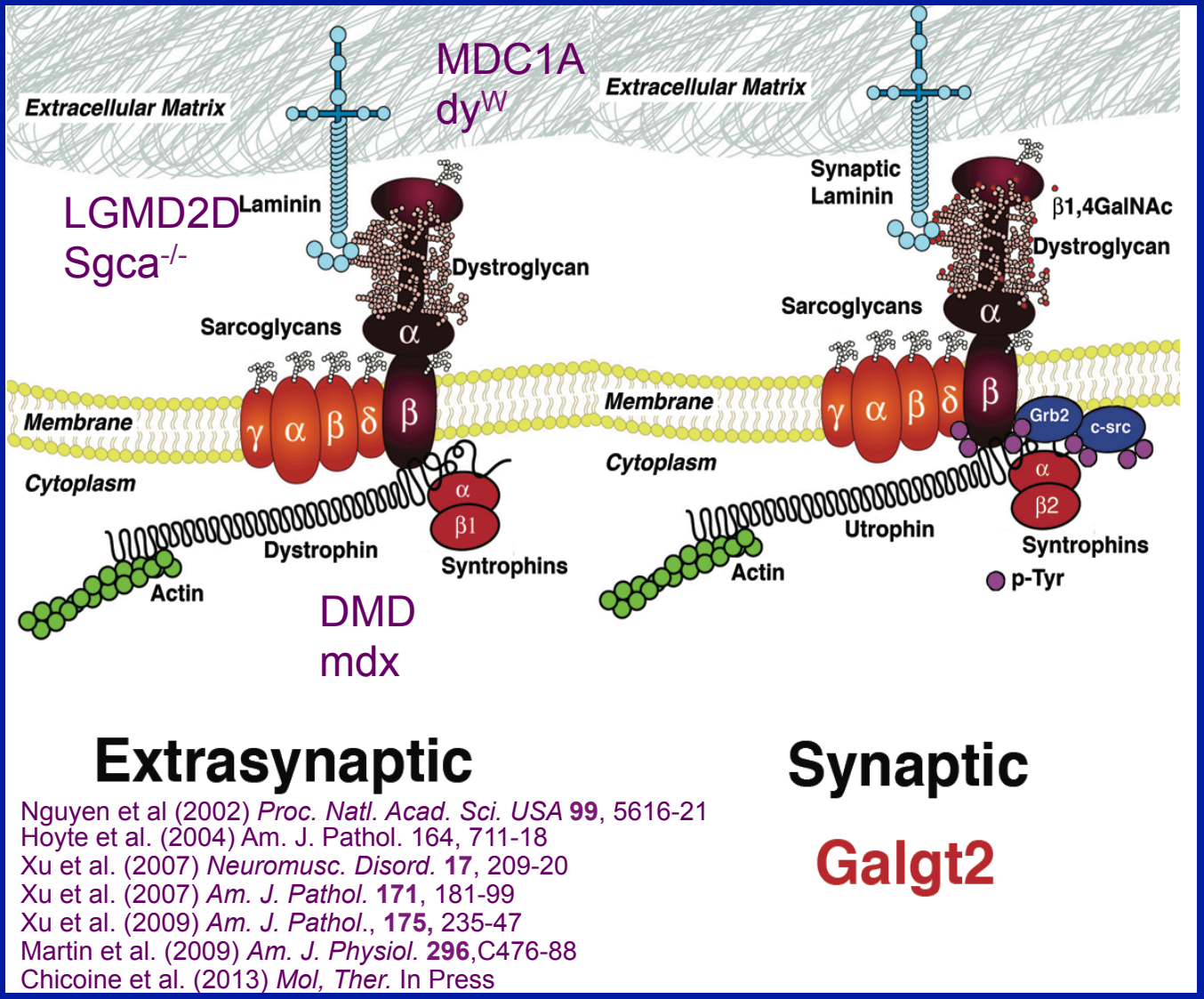



Nguyen et al (2002) *Proc. Natl. Acad. Sci. USA* **99**, 5616-21
Hoyte et al. (2004) Am. J. Pathol. 164, 711-18
Xu et al. (2007) *Neuromusc. Disord.* **17**, 209-20
Xu et al. (2007) *Am. J. Pathol.* **171**, 181-99
Xu et al. (2009) *Am. J. Pathol.*, **175,** 235-47
Martin et al. (2009) *Am. J. Physiol.* **296**,C476-88
Chicoine et al. (2013) *Mol, Ther.* In Press